EUROPEAN ORGANIZATION FOR NUCLEAR RESEARCH (CERN)

CERN-EP-2019-212
LHCb-PAPER-2019-031
December 22, 2019

Search for $A' \to \mu^+\mu^-$ decays

LHCb collaboration[†]

Abstract

Searches are performed for both prompt-like and long-lived dark photons, A', produced in proton-proton collisions at a center-of-mass energy of 13 TeV. These searches look for $A' \to \mu^+\mu^-$ decays using a data sample corresponding to an integrated luminosity of $5.5\,\text{fb}^{-1}$ collected with the LHCb detector. Neither search finds evidence for a signal, and 90% confidence-level exclusion limits are placed on the γ–A' kinetic-mixing strength. The prompt-like A' search explores the mass region from near the dimuon threshold up to 70 GeV, and places the most stringent constraints to date on dark photons with $214 < m(A') \lesssim 740\,\text{MeV}$ and $10.6 < m(A') \lesssim 30\,\text{GeV}$. The search for long-lived $A' \to \mu^+\mu^-$ decays places world-leading constraints on low-mass dark photons with lifetimes $\mathcal{O}(1)\,\text{ps}$.

Published as Physical Review Letters **124** (2020) 041801

[†]Authors are listed at the end of this Letter.

Substantial effort has been dedicated recently [1–3] to searching for the dark photon, A', a hypothetical massive vector boson that could mediate the interactions of dark matter particles [4], similar to how the ordinary photon, γ, mediates the electromagnetic (EM) interactions of charged Standard Model (SM) particles. The dark photon does not couple directly to SM particles; however, it can obtain a small coupling to the EM current due to kinetic mixing between the SM hypercharge and A' field strength tensors [5–12]. This coupling, which is suppressed relative to that of the photon by a factor labeled ε, would provide a portal through which dark photons can be produced in the laboratory, and also via which they can decay into visible SM final states. If the kinetic mixing arises due to processes described by one- or two-loop diagrams containing high-mass particles, possibly even at the Planck scale, then $10^{-12} \lesssim \varepsilon^2 \lesssim 10^{-4}$ is expected [2]. Exploring this *few-loop* ε region is one of the most important near-term goals of dark-sector physics.

Dark photons will decay into visible SM particles if invisible dark-sector decays are kinematically forbidden. Constraints have been placed on visible A' decays by previous beam-dump [12–28], fixed-target [29–32], collider [33–38], and rare-meson-decay [39–48] experiments. These experiments ruled out the few-loop region for dark-photon masses $m(A') \lesssim 10\,\text{MeV}$ ($c = 1$ throughout this Letter); however, most of the few-loop region at higher masses remains unexplored. Constraints on invisible A' decays can be found in Refs. [49–61]; only the visible scenario is considered here.

Many ideas have been proposed to further explore the $[m(A'), \varepsilon^2]$ parameter space [62–82]. The LHCb collaboration previously performed a search based on the approach proposed in Ref. [76] using data corresponding to $1.6\,\text{fb}^{-1}$ collected in 2016 [83]. The constraints placed on prompt-like dark photons, where the dark-photon lifetime is small compared to the detector resolution, were the most stringent to date for $10.6 < m(A') < 70\,\text{GeV}$ and comparable to the best existing limits for $m(A') < 0.5\,\text{GeV}$. The search for long-lived dark photons was the first to achieve sensitivity using a displaced-vertex signature, though only small regions of $[m(A'), \varepsilon^2]$ parameter space were excluded.

This Letter presents searches for both prompt-like and long-lived dark photons produced in proton-proton, pp, collisions at a center-of-mass energy of 13 TeV, looking for $A' \to \mu^+\mu^-$ decays using a data sample corresponding to an integrated luminosity of $5.5\,\text{fb}^{-1}$ collected with the LHCb detector in 2016–2018. The strategies employed in these searches are the same as in Ref. [83], though the three-fold increase in integrated luminosity, improved trigger efficiency during 2017–2018 data taking, and improvements in the analysis provide much better sensitivity to dark photons. The prompt-like A' search is performed from near the dimuon threshold up to 70 GeV, achieving a factor of 5 (2) better sensitivity to ε^2 at low (high) masses than Ref. [83]. The long-lived A' search is restricted to the mass range $214 < m(A') < 350\,\text{MeV}$, where the data sample potentially has sensitivity, and provides access to much larger regions of $[m(A'), \varepsilon^2]$ parameter space.

Both the production and decay kinematics of the $A' \to \mu^+\mu^-$ and $\gamma^* \to \mu^+\mu^-$ processes are identical, since dark photons produced in pp collisions via γ–A' mixing inherit the production mechanisms of off-shell photons with $m(\gamma^*) = m(A')$. Furthermore, the expected $A' \to \mu^+\mu^-$ signal yield is related to the observed prompt $\gamma^* \to \mu^+\mu^-$ yield in a small $\pm\Delta m$ window around $m(A')$, $n_{\text{ob}}^{\gamma^*}[m(A')]$, by [76]

$$n_{\text{ex}}^{A'}[m(A'), \varepsilon^2] = \varepsilon^2 \left[\frac{n_{\text{ob}}^{\gamma^*}[m(A')]}{2\Delta m}\right] \mathcal{F}[m(A')]\, \epsilon_{\gamma^*}^{A'}[m(A'), \tau(A')], \tag{1}$$

where the dark-photon lifetime, $\tau(A')$, is a known function of $m(A')$ and ε^2, $\mathcal{F}$ is a

known $m(A')$-dependent function, and $\epsilon^{A'}_{\gamma^*}[m(A'),\tau(A')]$ is the $\tau(A')$-dependent ratio of the $A'\to\mu^+\mu^-$ and $\gamma^*\to\mu^+\mu^-$ detection efficiencies. For prompt-like dark photons, $A'\to\mu^+\mu^-$ decays are experimentally indistinguishable from prompt $\gamma^*\to\mu^+\mu^-$ decays, resulting in $\epsilon^{A'}_{\gamma^*}[m(A'),\tau(A')]=1$. This facilitates a fully data-driven search where most experimental systematic effects cancel, since the observed $A'\to\mu^+\mu^-$ yields, $n^{A'}_{\rm ob}[m(A')]$, can be normalized to $n^{A'}_{\rm ex}[m(A'),\varepsilon^2]$ to obtain constraints on ε^2 without any knowledge of the detector efficiency or luminosity. When $\tau(A')$ is larger than the detector decay-time resolution, $A'\to\mu^+\mu^-$ decays can potentially be reconstructed as displaced from the primary pp vertex (PV) resulting in $\epsilon^{A'}_{\gamma^*}[m(A'),\tau(A')]\neq 1$; however, only the $\tau(A')$ dependence of the detection efficiency is required to use Eq. (1). Finally, Eq. (1) is altered for large $m(A')$ to account for additional kinetic mixing with the Z boson [84, 85].

The LHCb detector is a single-arm forward spectrometer covering the pseudorapidity range $2<\eta<5$, described in detail in Refs. [86, 87]. The prompt-like A' search is based on a data sample that employs a novel data-storage strategy, made possible by advances in the LHCb data-taking scheme introduced in 2015 [88, 89], where all online-reconstructed particles are stored, but most lower-level information is discarded, greatly reducing the event size. In contrast, the data sample used in the long-lived A' search is derived from the standard LHCb data stream. Simulated data samples, which are used to validate the analysis, are produced using the software described in Refs. [90–92].

The online event selection is performed by a trigger [93] consisting of a hardware stage using information from the calorimeter and muon systems, followed by a software stage that performs a full event reconstruction. At the hardware stage, events are required to have a muon with momentum transverse to the beam direction $p_{\rm T}(\mu)\gtrsim 1.8\,{\rm GeV}$, or a dimuon pair with $p_{\rm T}(\mu^+)p_{\rm T}(\mu^-)\gtrsim(1.5\,{\rm GeV})^2$. The long-lived A' search also uses events selected at the hardware stage due to the presence of a high-$p_{\rm T}$ hadron that is not associated to the $A'\to\mu^+\mu^-$ candidate. In the software stage, where the $p_{\rm T}$ resolution is substantially improved *cf.* the hardware stage, $A'\to\mu^+\mu^-$ candidates are built from two oppositely charged tracks that form a good-quality vertex and satisfy stringent muon-identification criteria, though these criteria were loosened considerably in the low-mass region during 2017–2018 data taking. Both searches require $p_{\rm T}(A')>1\,{\rm GeV}$ and $2<\eta(\mu)<4.5$. The prompt-like A' search uses muons that are consistent with originating from the PV, with $p_{\rm T}(\mu)>1.0\,{\rm GeV}$ and momentum $p(\mu)>20\,{\rm GeV}$ in 2016, and $p_{\rm T}(\mu)>0.5\,{\rm GeV}$, $p(\mu)>10\,{\rm GeV}$, and $p_{\rm T}(\mu^+)p_{\rm T}(\mu^-)>(1.0\,{\rm GeV})^2$ in 2017–2018. The long-lived A' search uses muons that are inconsistent with originating from any PV with $p_{\rm T}(\mu)>0.5\,{\rm GeV}$ and $p(\mu)>10\,{\rm GeV}$, and requires $2<\eta(A')<4.5$ and a decay topology consistent with a dark photon originating from a PV.

The prompt-like A' sample is contaminated by prompt $\gamma^*\to\mu^+\mu^-$ production, various resonant decays to $\mu^+\mu^-$, whose mass-peak regions are avoided in the search, and by the following types of misreconstruction: (hh) two prompt hadrons misidentified as muons; $(h\mu_Q)$ a misidentified prompt hadron combined with a muon produced in the decay of a heavy-flavor quark, Q, that is misidentified as prompt; and $(\mu_Q\mu_Q)$ two muons produced in Q-hadron decays that are both misidentified as prompt. Contamination from a prompt muon and a misidentified prompt hadron is negligible, though it is accounted for automatically by the method used to determine the sum of the hh and $h\mu_Q$ contributions. The impact of the $\gamma^*\to\mu^+\mu^-$ background is reduced, *cf.* Ref. [83], by constraining the muons to originate from the PV when determining $m(\mu^+\mu^-)$. This improves the resolution, $\sigma[m(\mu^+\mu^-)]$, by about a factor of 2 for small $m(A')$. The misreconstructed backgrounds

are highly suppressed by the stringent requirements applied in the trigger; however, substantial contributions remain for $m(A') \gtrsim 1.1\,\text{GeV}$. In this mass region, dark photons are expected to be predominantly produced in Drell–Yan processes, from which they would inherit the well-known signature of dimuon pairs that are largely isolated. Therefore, the signal sensitivity is enhanced by applying the anti-k_{T}-based [94–96] isolation requirement described in Refs. [83, 97] for $m(A') > 1.1\,\text{GeV}$.

The observed prompt-like $A' \to \mu^+\mu^-$ yields, which are determined from fits to the $m(\mu^+\mu^-)$ spectrum, are normalized using Eq. (1) to obtain constraints on ε^2. The $n_{\text{ob}}^{\gamma^*}[m(A')]$ values in Eq. (1) are obtained from binned extended maximum likelihood fits to the $\min[\chi^2_{\text{IP}}(\mu^\pm)]$ distributions, where $\chi^2_{\text{IP}}(\mu)$ is defined as the difference in the vertex-fit χ^2 when the PV is reconstructed with and without the muon. The $\min[\chi^2_{\text{IP}}(\mu^\pm)]$ distribution provides excellent discrimination between prompt muons and the displaced muons that constitute the $\mu_Q\mu_Q$ background. The $\chi^2_{\text{IP}}(\mu)$ quantity approximately follows a χ^2 probability density function (PDF), with two degrees of freedom, and therefore, the $\min[\chi^2_{\text{IP}}(\mu^\pm)]$ distributions have minimal dependence on mass for each source of dimuon candidates. The prompt-dimuon PDFs are taken directly from data at $m(J/\psi)$ and $m(Z)$, where prompt resonances are dominant. Small corrections are applied to obtain these PDFs at all other $m(A')$, which are validated near threshold, at $m(\phi)$, and at $m[\Upsilon(1S)]$, where the data predominantly consist of prompt dimuon pairs. Based on these validation studies, a shape uncertainty of 2% is applied in each $\min[\chi^2_{\text{IP}}(\mu^\pm)]$ bin. Same-sign $\mu^\pm\mu^\pm$ candidates provide estimates for the PDF and yield of the sum of the hh and $h\mu_Q$ contributions, where each involves misidentified prompt hadrons. The $\mu^\pm\mu^\pm$ yields are corrected to account for the difference in the production rates of $\pi^+\pi^-$ and $\pi^\pm\pi^\pm$, which are determined precisely from data using dipion candidates weighted to account for the kinematic dependence of the muon misidentification probability, since the hh background largely consists of $\pi^+\pi^-$ pairs where both pions are misidentified. The uncertainty due to the finite size of the $\mu^\pm\mu^\pm$ sample in each bin is included in the likelihood. Simulated Q-hadron decays are used to obtain the $\mu_Q\mu_Q$ PDFs, where the dominant uncertainties are from the relative importance of the various Q-hadron decay contributions at each mass. Example $\min[\chi^2_{\text{IP}}(\mu^\pm)]$ fits are provided in Ref. [97], while the resulting prompt-like candidate categorization versus $m(\mu^+\mu^-)$ is shown in Fig. 1. Finally, the $n_{\text{ob}}^{\gamma^*}[m(A')]$ yields are corrected for bin migration due to bremsstrahlung, which is negligible except near the low-mass tails of the J/ψ and $\Upsilon(1S)$, and the small expected Bethe–Heitler contribution is subtracted [76], resulting in the $n_{\text{ex}}^{A'}[m(A'), \varepsilon^2]$ values shown in Fig. S2 of Ref. [97].

The prompt-like $n_{\text{ob}}^{A'}[m(A')]$ mass spectrum is scanned in steps of $\sigma[m(\mu^+\mu^-)]/2$ searching for $A' \to \mu^+\mu^-$ contributions [97], using the strategy from Ref. [83]. At each mass, a binned extended maximum likelihood fit is performed in a $\pm 12.5\,\sigma[m(\mu^+\mu^-)]$ window around $m(A')$. The profile likelihood is used to determine the p-value and the upper limit at 90% confidence level (CL) on $n_{\text{ob}}^{A'}[m(A')]$. The signal is well modeled by a Gaussian distribution whose resolution is determined with 10% precision using a combination of simulated $A' \to \mu^+\mu^-$ decays and the observed p_{T}-dependent widths of the large resonance peaks in the data. The mass-resolution uncertainty is included in the profile likelihood. The method of Ref. [98] selects the background model from a large set of potential components, which includes all Legendre modes up to tenth order and dedicated terms for known resonances, by performing a data-driven process whose uncertainty is included in the profile likelihood following Ref. [99]. No significant excess is found in the prompt-like $m(A')$ spectrum, after accounting for the trials factor due to the number of

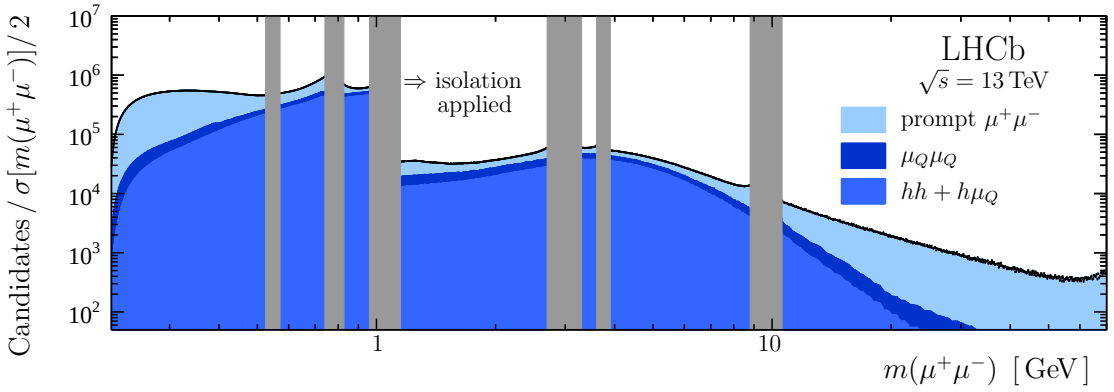

Figure 1: Prompt-like mass spectrum, where the categorization of the data as prompt $\mu^+\mu^-$, $\mu_Q\mu_Q$, and $hh + h\mu_Q$ is determined using the $\min[\chi^2_{\rm IP}(\mu^\pm)]$ fits described in the text (examples of these fits are provided in the Supplemental Material). The anti-$k_{\rm T}$-based isolation requirement is applied for $m(A') > 1.1\,\text{GeV}$.

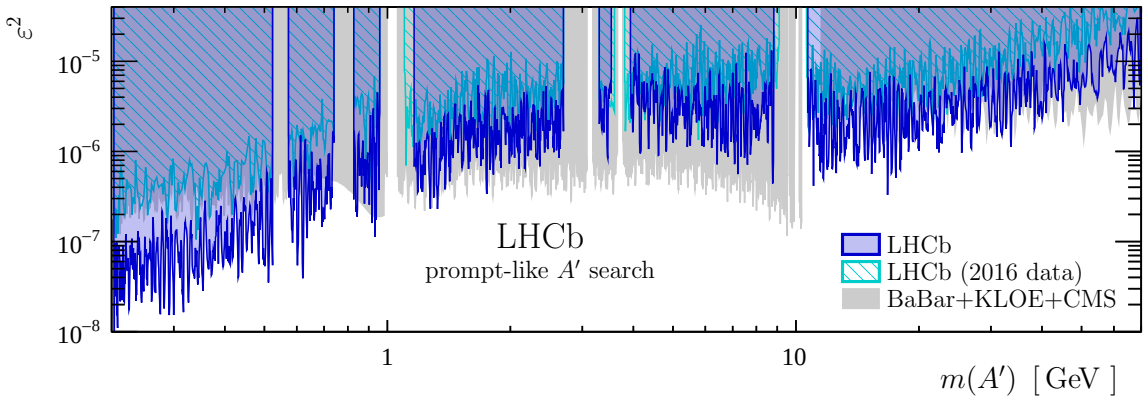

Figure 2: Regions of the $[m(A'), \varepsilon^2]$ parameter space excluded at 90% CL by the prompt-like A' search compared to the best published [35, 38, 83] and preliminary [102] limits.

signal hypotheses.

Dark photons are excluded at 90% CL where the upper limit on $n^{A'}_{\rm ob}[m(A')]$ is less than $n^{A'}_{\rm ex}[m(A'), \varepsilon^2]$. Figure 2 shows that the constraints placed on prompt-like dark photons are the most stringent for $214 < m(A') \lesssim 740\,\text{MeV}$ and $10.6 < m(A') \lesssim 30\,\text{GeV}$. The low-mass constraints are the strongest placed by a prompt-like A' search at any $m(A')$. These results are corrected for inefficiency and changes in the mass resolution that arise due to $\tau(A')$ no longer being negligible at such small values of ϵ^2. The high-mass constraints are adjusted to account for additional kinetic mixing with the Z boson [84, 85], which alters Eq. (1). Since the LHCb detector response is independent of which $q\bar{q} \to A'$ process produces the dark photon above 10 GeV, it is straightforward to recast the results in Fig. 2 for other models [100, 101].

For the long-lived A' search, contamination from prompt particles is negligible due to a stringent criterion applied in the trigger on $\min[\chi^2_{\rm IP}(\mu^\pm)]$ that requires muons be inconsistent with originating from any PV. Therefore, the dominant background contributions

are: photons that convert into $\mu^+\mu^-$ in the silicon-strip vertex detector that surrounds the pp interaction region, known as the VELO [103]; b-hadron decay chains that produce two muons; and the low-mass tail from $K^0_{\rm S} \to \pi^+\pi^-$ decays, where both pions are misidentified as muons (all other strange decays are negligible). A p-value is assigned to the photon-conversion hypothesis for each long-lived $A' \to \mu^+\mu^-$ candidate using properties of the decay vertex and muon tracks, along with a high-precision three-dimensional material map produced from a data sample of secondary hadronic interactions [104]. A $m(A')$-dependent requirement is applied to these p-values that results in conversions having negligible impact on the sensitivity, though they are still accounted for to prevent pathologies when there are no other background sources. The remaining backgrounds are highly suppressed by the decay topology requirement applied in the trigger. Furthermore, since muons produced in b-hadron decays are often accompanied by additional displaced tracks, events are rejected if they are selected by the inclusive heavy-flavor software trigger [105, 106] independently of the presence of the $A' \to \mu^+\mu^-$ candidate. In addition, boosted decision tree classifiers are used to reject events containing tracks consistent with originating from the same b-hadron decay as the signal muon candidates [107].

The long-lived A' search is also normalized using Eq. (1); however, $\epsilon^{A'}_{\gamma^*}[m(A'), \tau(A')]$ is not unity, in part because the efficiency depends on the decay time, t. The kinematics are identical for $A' \to \mu^+\mu^-$ and prompt $\gamma^* \to \mu^+\mu^-$ decays for $m(A') = m(\gamma^*)$; therefore, the t dependence of $\epsilon^{A'}_{\gamma^*}[m(A'), \tau(A')]$ is obtained by resampling prompt $\gamma^* \to \mu^+\mu^-$ candidates as long-lived $A' \to \mu^+\mu^-$ decays, where all t-dependent properties, *e.g.* $\min[\chi^2_{\rm IP}(\mu^\pm)]$, are recalculated based on the resampled decay-vertex locations (the impact of background contamination in the prompt $\gamma^* \to \mu^+\mu^-$ sample is negligible). This approach is validated using simulation, where prompt $A' \to \mu^+\mu^-$ decays are used to predict the properties of long-lived $A' \to \mu^+\mu^-$ decays. The relative uncertainty on $\epsilon^{A'}_{\gamma^*}[m(A'), \tau(A')]$ is estimated to be 5%, which arises largely due to limited knowledge of how radiation damage affects the performance of the VELO as a function of the distance from the pp interaction region. The looser kinematic, muon-identification, and hardware-trigger requirements applied to long-lived $A' \to \mu^+\mu^-$ candidates, *cf.* prompt-like candidates, also increase the efficiency. This t-independent increase in efficiency is determined using a control data sample of dimuon candidates consistent with originating from the PV, but otherwise satisfying the long-lived criteria. The $n^{A'}_{\rm ex}[m(A'), \varepsilon^2]$ values obtained using these data-driven $\epsilon^{A'}_{\gamma^*}[m(A'), \tau(A')]$ values (discussed in more detail in Ref. [97]), along with the expected prompt-like $A' \to \mu^+\mu^-$ yields, are shown in Fig. 3.

The long-lived $m(A')$ spectrum is also scanned in discrete steps of $\sigma[m(\mu^+\mu^-)]/2$ looking for $A' \to \mu^+\mu^-$ contributions [97]; however, discrete steps in $\tau(A')$ are also considered here. Binned extended maximum likelihood fits are performed to the three-dimensional feature space of $m(\mu^+\mu^-)$, t, and the consistency of the decay topology as quantified in the decay-fit $\chi^2_{\rm DF}$, which has three degrees of freedom. The photon-conversion contribution is derived in each $[m(\mu^+\mu^-), t, \chi^2_{\rm DF}]$ bin from the number of dimuon candidates that are rejected by the conversion criterion. Both the b-hadron and $K^0_{\rm S}$ contributions are modeled in each $[t, \chi^2_{\rm DF}]$ bin by second-order polynomials of the energy released in the decay, $\sqrt{m(\mu^+\mu^-)^2 - 4m(\mu)^2}$. These contributions are validated using the following large control data samples: candidates that fail the b-hadron suppression requirements; and candidates that fail, but nearly satisfy, the stringent muon-identification requirements. The profile likelihood is used to obtain the p-values and confidence intervals on $n^{A'}_{\rm ob}[m(A'), \tau(A')]$. No significant excess is observed in the long-lived $A' \to \mu^+\mu^-$ search (the three-dimensional

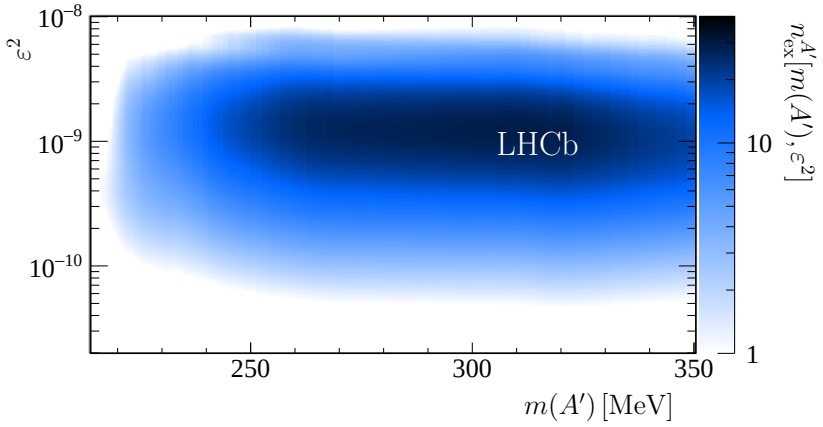

Figure 3: Expected reconstructed and selected long-lived $A' \to \mu^+\mu^-$ yield.

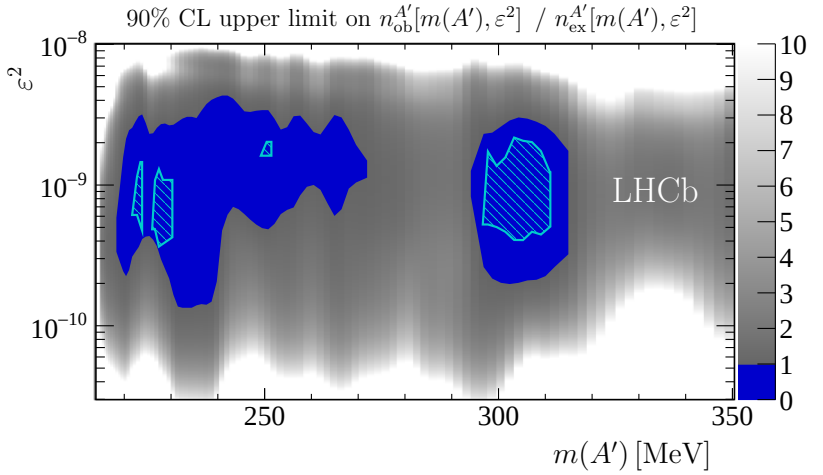

Figure 4: Ratio of the observed upper limit on $n_{\rm ob}^{A'}[m(A'),\varepsilon^2]$ at 90% CL to the expected dark-photon yield, $n_{\rm ex}^{A'}[m(A'),\varepsilon^2]$, where regions less than unity are excluded. The only constraints in this region are from (hashed) the previous LHCb search [83].

data distribution and the background-only pull distributions are provided in Ref. [97]).

Since the relationship between $\tau(A')$ and ε^2 is known at each mass [76], the upper limits on $n_{\rm ob}^{A'}[m(A'),\tau(A')]$ are easily translated into limits on $n_{\rm ob}^{A'}[m(A'),\varepsilon^2]$. Regions of the $[m(A'),\varepsilon^2]$ parameter space where the upper limit on $n_{\rm ob}^{A'}[m(A'),\varepsilon^2]$ is less than $n_{\rm ex}^{A'}[m(A'),\varepsilon^2]$ are excluded at 90% CL. Figure 4 shows that sizable regions of $[m(A'),\varepsilon^2]$ parameter space are excluded, which are much larger than those excluded in Ref. [83].

In summary, searches are performed for prompt-like and long-lived dark photons produced in pp collisions at a center-of-mass energy of 13 TeV. Both searches look for $A' \to \mu^+\mu^-$ decays using a data sample corresponding to an integrated luminosity of 5.5 fb^{-1} collected with the LHCb detector during 2016–2018. No evidence for a signal is found in either search, and 90% CL exclusion regions are set on the γ–A' kinetic-mixing strength. The prompt-like A' search is performed from near the dimuon threshold up to 70 GeV, and produces the most stringent constraints on dark photons with $214 < m(A') \lesssim 740$ MeV and $10.6 < m(A') \lesssim 30$ GeV. The long-lived A' search is restricted to the mass range

$214 < m(A') < 350\,\text{MeV}$, where the data sample potentially has sensitivity, and places world-leading constraints on low-mass dark photons with lifetimes $\mathcal{O}(1)\,\text{ps}$. The three-fold increase in integrated luminosity, improved trigger efficiency during 2017–2018 data taking, and improvements in the analysis result in the searches presented in this Letter achieving much better sensitivity to dark photons than the previous LHCb results [83]. The prompt-like A' search achieves a factor of 5 (2) better sensitivity to ε^2 at low (high) masses than Ref. [83], while the long-lived A' search provides access to much larger regions of $[m(A'), \varepsilon^2]$ parameter space.

These results demonstrate the excellent sensitivity of the LHCb experiment to dark photons, even using a data sample collected with a hardware-trigger stage that is highly inefficient for low-mass $A' \to \mu^+\mu^-$ decays. The removal of this hardware-trigger stage in Run 3, along with the planned increase in luminosity, should increase the potential yield of $A' \to \mu^+\mu^-$ decays in the low-mass region by a factor $\mathcal{O}(100)$ compared to the 2016–2018 data sample. Given that most of the parameter space shown in Fig. 4 would have been accessible if the data sample was only three times larger, these upgrades will greatly increase the dark-photon discovery potential of the LHCb experiment.

Acknowledgements

We express our gratitude to our colleagues in the CERN accelerator departments for the excellent performance of the LHC. We thank the technical and administrative staff at the LHCb institutes. We acknowledge support from CERN and from the national agencies: CAPES, CNPq, FAPERJ and FINEP (Brazil); MOST and NSFC (China); CNRS/IN2P3 (France); BMBF, DFG and MPG (Germany); INFN (Italy); NWO (Netherlands); MNiSW and NCN (Poland); MEN/IFA (Romania); MSHE (Russia); MinECo (Spain); SNSF and SER (Switzerland); NASU (Ukraine); STFC (United Kingdom); DOE NP and NSF (USA). We acknowledge the computing resources that are provided by CERN, IN2P3 (France), KIT and DESY (Germany), INFN (Italy), SURF (Netherlands), PIC (Spain), GridPP (United Kingdom), RRCKI and Yandex LLC (Russia), CSCS (Switzerland), IFIN-HH (Romania), CBPF (Brazil), PL-GRID (Poland) and OSC (USA). We are indebted to the communities behind the multiple open-source software packages on which we depend. Individual groups or members have received support from AvH Foundation (Germany); EPLANET, Marie Skłodowska-Curie Actions and ERC (European Union); ANR, Labex P2IO and OCEVU, and Région Auvergne-Rhône-Alpes (France); Key Research Program of Frontier Sciences of CAS, CAS PIFI, and the Thousand Talents Program (China); RFBR, RSF and Yandex LLC (Russia); GVA, XuntaGal and GENCAT (Spain); the Royal Society and the Leverhulme Trust (United Kingdom).

References

[1] R. Essig *et al.*, *Working Group Report: New light weakly coupled particles*, in *Proceedings, 2013 Community Summer Study on the Future of U.S. Particle Physics: Snowmass on the Mississippi (CSS2013): Minneapolis, MN, USA, July 29-August 6, 2013*, 2013, arXiv:1311.0029.

[2] J. Alexander *et al.*, *Dark Sectors 2016 Workshop: Community Report*, 2016, arXiv:1608.08632.

[3] M. Battaglieri *et al.*, *US Cosmic Visions: New Ideas in Dark Matter 2017: Community Report*, arXiv:1707.04591.

[4] S. Tulin and H.-B. Yu, *Dark matter self-interactions and small scale structure*, Phys. Rept. **730** (2018) 1, arXiv:1705.02358.

[5] P. Fayet, *On the search for a new spin 1 boson*, Nucl. Phys. **B187** (1981) 184.

[6] P. Fayet, *Effects of the spin 1 partner of the goldstino (gravitino) on neutral current phenomenology*, Phys. Lett. **95B** (1980) 285.

[7] L. B. Okun, *Limits of electrodynamics: Paraphotons?*, Sov. Phys. JETP **56** (1982) 502, [Zh. Eksp. Teor. Fiz. **83** (1982) 892].

[8] P. Galison and A. Manohar, *Two Z's or not two Z's?*, Phys. Lett. **B136** (1984) 279.

[9] B. Holdom, *Two $U(1)$'s and ϵ charge shifts*, Phys. Lett. **B166** (1986) 196.

[10] M. Pospelov, A. Ritz, and M. B. Voloshin, *Secluded WIMP dark matter*, Phys. Lett. **B662** (2008) 53, arXiv:0711.4866.

[11] N. Arkani-Hamed, D. P. Finkbeiner, T. R. Slatyer, and N. Weiner, *A theory of dark matter*, Phys. Rev. **D79** (2009) 015014, arXiv:0810.0713.

[12] J. D. Bjorken, R. Essig, P. Schuster, and N. Toro, *New fixed-target experiments to search for dark gauge forces*, Phys. Rev. **D80** (2009) 075018, arXiv:0906.0580.

[13] CHARM collaboration, F. Bergsma *et al.*, *A search for decays of heavy neutrinos in the mass range 0.5 GeV to 2.8 GeV*, Phys. Lett. **B166** (1986) 473.

[14] A. Konaka *et al.*, *Search for neutral particles in electron-beam-dump experiment*, Phys. Rev. Lett. **57** (1986) 659.

[15] E. M. Riordan *et al.*, *Search for short-lived axions in an electron-beam-dump experiment*, Phys. Rev. Lett. **59** (1987) 755.

[16] J. D. Bjorken, S. Ecklund, W. R. Nelson, A. Abashian, C. Church, B. Lu, L. W. Mo, T. A. Nunamaker, and P. Rassmann, *Search for neutral metastable penetrating particles produced in the SLAC beam dump*, Phys. Rev. **D38** (1988) 3375.

[17] A. Bross, M. Crisler, S. H. Pordes, J. Volk, S. Errede, and J. Wrbanek, *A search for short-lived particles produced in an electron beam dump*, Phys. Rev. Lett. **67** (1991) 2942.

[18] M. Davier and H. Nguyen Ngoc, *An unambiguous search for a light Higgs boson*, Phys. Lett. **B229** (1989) 150.

[19] LSND collaboration, C. Athanassopoulos *et al.*, *Evidence for $\nu_\mu \to \nu_e$ oscillations from pion decay in flight neutrinos*, Phys. Rev. **C58** (1998) 2489, arXiv:nucl-ex/9706006.

[20] NOMAD collaboration, P. Astier *et al.*, *Search for heavy neutrinos mixing with tau neutrinos*, Phys. Lett. **B506** (2001) 27, arXiv:hep-ex/0101041.

[21] R. Essig, R. Harnik, J. Kaplan, and N. Toro, *Discovering new light states at neutrino experiments*, Phys. Rev. **D82** (2010) 113008, arXiv:1008.0636.

[22] M. Williams, C. P. Burgess, A. Maharana, and F. Quevedo, *New constraints (and motivations) for abelian gauge bosons in the MeV-TeV mass range*, JHEP **08** (2011) 106, arXiv:1103.4556.

[23] J. Blümlein and J. Brunner, *New exclusion limits for dark gauge forces from beam-dump data*, Phys. Lett. **B701** (2011) 155, arXiv:1104.2747.

[24] S. N. Gninenko, *Constraints on sub-GeV hidden sector gauge bosons from a search for heavy neutrino decays*, Phys. Lett. **B713** (2012) 244, arXiv:1204.3583.

[25] J. Blümlein and J. Brunner, *New exclusion limits on dark gauge forces from proton bremsstrahlung in beam-dump data*, Phys. Lett. **B731** (2014) 320, arXiv:1311.3870.

[26] NA64 collaboration, D. Banerjee *et al.*, *Search for a hypothetical 16.7 MeV gauge boson and dark photons in the NA64 experiment at CERN*, Phys. Rev. Lett. **120** (2018) 231802, arXiv:1803.07748.

[27] S. Andreas, C. Niebuhr, and A. Ringwald, *New limits on hidden photons from past electron beam dumps*, Phys. Rev. **D86** (2012) 095019, arXiv:1209.6083.

[28] CHARM collaboration, F. Bergsma *et al.*, *Search for axion like particle production in 400-GeV proton-copper interactions*, Phys. Lett. **157B** (1985) 458.

[29] APEX collaboration, S. Abrahamyan *et al.*, *Search for a new gauge boson in electron-nucleus fixed-target scattering by the APEX experiment*, Phys. Rev. Lett. **107** (2011) 191804, arXiv:1108.2750.

[30] A1 collaboration, H. Merkel *et al.*, *Search at the Mainz Microtron for light massive gauge bosons relevant for the muon g-2 anomaly*, Phys. Rev. Lett. **112** (2014) 221802, arXiv:1404.5502.

[31] A1 collaboration, H. Merkel *et al.*, *Search for light gauge bosons of the dark sector at the Mainz Microtron*, Phys. Rev. Lett. **106** (2011) 251802, arXiv:1101.4091.

[32] HPS collaboration, P. H. Adrian *et al.*, *Search for a dark photon in electroproduced e^+e^- pairs with the Heavy Photon Search experiment at JLab*, Phys. Rev. **D98** (2018) 091101, arXiv:1807.11530.

[33] BaBar collaboration, B. Aubert *et al.*, *Search for dimuon decays of a light scalar boson in radiative transitions $\Upsilon \to \gamma A^0$*, Phys. Rev. Lett. **103** (2009) 081803, arXiv:0905.4539.

[34] D. Curtin *et al.*, *Exotic decays of the 125 GeV Higgs boson*, Phys. Rev. **D90** (2014) 075004, arXiv:1312.4992.

[35] BaBar collaboration, J. P. Lees *et al.*, *Search for a dark photon in e^+e^- collisions at BaBar*, Phys. Rev. Lett. **113** (2014) 201801, arXiv:1406.2980.

[36] BESIII collaboration, M. Ablikim *et al.*, *Dark photon search in the mass range between 1.5 and 3.4 GeV/c^2*, Phys. Lett. **B774** (2017) 252, arXiv:1705.04265.

[37] KLOE-2 collaboration, A. Anastasi *et al.*, *Limit on the production of a low-mass vector boson in $e^+e^- \to U\gamma$, $U \to e^+e^-$ with the KLOE experiment*, Phys. Lett. **B750** (2015) 633, arXiv:1509.00740.

[38] KLOE-2 collaboration, A. Anastasi *et al.*, *Combined limit on the production of a light gauge boson decaying into $\mu^+\mu^-$ and $\pi^+\pi^-$*, Phys. Lett. **B784** (2018) 336, arXiv:1807.02691.

[39] G. Bernardi *et al.*, *Search for neutrino decay*, Phys. Lett. **B166** (1986) 479.

[40] SINDRUM I collaboration, R. Meijer Drees *et al.*, *Search for weakly interacting neutral bosons produced in π^-p interactions at rest and decaying into e^+e^- pairs*, Phys. Rev. Lett. **68** (1992) 3845.

[41] KLOE-2 collaboration, F. Archilli *et al.*, *Search for a vector gauge boson in ϕ meson decays with the KLOE detector*, Phys. Lett. **B706** (2012) 251, arXiv:1110.0411.

[42] S. N. Gninenko, *Stringent limits on the $\pi^0 \to \gamma X, X \to e^+e^-$ decay from neutrino experiments and constraints on new light gauge bosons*, Phys. Rev. **D85** (2012) 055027, arXiv:1112.5438.

[43] KLOE-2 collaboration, D. Babusci *et al.*, *Limit on the production of a light vector gauge boson in ϕ meson decays with the KLOE detector*, Phys. Lett. **B720** (2013) 111, arXiv:1210.3927.

[44] WASA-at-COSY collaboration, P. Adlarson *et al.*, *Search for a dark photon in the $\pi^0 \to e^+e^-\gamma$ decay*, Phys. Lett. **B726** (2013) 187, arXiv:1304.0671.

[45] HADES collaboration, G. Agakishiev *et al.*, *Searching a dark photon with HADES*, Phys. Lett. **B731** (2014) 265, arXiv:1311.0216.

[46] PHENIX collaboration, A. Adare *et al.*, *Search for dark photons from neutral meson decays in pp and dAu collisions at $\sqrt{s_{NN}} = 200$ GeV*, Phys. Rev. **C91** (2015) 031901, arXiv:1409.0851.

[47] NA48/2 collaboration, J. R. Batley *et al.*, *Search for the dark photon in π^0 decays*, Phys. Lett. **B746** (2015) 178, arXiv:1504.00607.

[48] KLOE-2 collaboration, A. Anastasi *et al.*, *Limit on the production of a new vector boson in $e^+e^- \to U\gamma$, $U \to \pi^+\pi^-$ with the KLOE experiment*, Phys. Lett. **B757** (2016) 356, arXiv:1603.06086.

[49] R. Essig, J. Mardon, M. Papucci, T. Volansky, and Y.-M. Zhong, *Constraining light dark matter with low-energy e^+e^- colliders*, JHEP **11** (2013) 167, arXiv:1309.5084.

[50] H. Davoudiasl, H.-S. Lee, and W. J. Marciano, *Muon $g-2$, rare kaon decays, and parity violation from dark bosons*, Phys. Rev. **D89** (2014) 095006, arXiv:1402.3620.

[51] NA64 collaboration, D. Banerjee *et al.*, *Search for invisible decays of sub-GeV dark photons in missing-energy events at the CERN SPS*, Phys. Rev. Lett. **118** (2017) 011802, arXiv:1610.02988.

[52] BaBar collaboration, J. P. Lees *et al.*, *Search for invisible decays of a dark photon produced in e^+e^- collisions at BaBar*, Phys. Rev. Lett. **119** (2017) 131804, arXiv:1702.03327.

[53] E787 collaboration, S. Adler *et al.*, *Further evidence for the decay $K^+ \to \pi^+\nu\bar{\nu}$*, Phys. Rev. Lett. **88** (2002) 041803, arXiv:hep-ex/0111091.

[54] E787 collaboration, S. Adler *et al.*, *Further search for the decay $K^+ \to \pi^+\nu\bar{\nu}$ in the momentum region $p < 195$ MeV/c*, Phys. Rev. **D70** (2004) 037102, arXiv:hep-ex/0403034.

[55] BNL-E949 collaboration, A. V. Artamonov *et al.*, *Study of the decay $K^+ \to \pi^+\nu\bar{\nu}$ in the momentum region $140 < P_\pi < 199$ MeV/c*, Phys. Rev. **D79** (2009) 092004, arXiv:0903.0030.

[56] P. Fayet, *Constraints on light dark matter and U bosons, from ψ, Υ, K^+, π^0, η and η' decays*, Phys. Rev. **D74** (2006) 054034, arXiv:hep-ph/0607318.

[57] P. Fayet, *U-boson production in e^+e^- annihilations, ψ and Υ decays, and light dark matter*, Phys. Rev. **D75** (2007) 115017, arXiv:hep-ph/0702176.

[58] P. J. Fox, R. Harnik, J. Kopp, and Y. Tsai, *LEP shines light on dark matter*, Phys. Rev. **D84** (2011) 014028, arXiv:1103.0240.

[59] NA62 collaboration, E. Cortina Gil *et al.*, *Search for production of an invisible dark photon in π^0 decays*, JHEP **05** (2019) 182, arXiv:1903.08767.

[60] DELPHI collaboration, J. Abdallah *et al.*, *Photon events with missing energy in e^+e^- collisions at $\sqrt{s} = 130$-GeV to 209-GeV*, Eur. Phys. J. **C38** (2005) 395, arXiv:hep-ex/0406019.

[61] DELPHI collaboration, J. Abdallah *et al.*, *Search for one large extra dimension with the DELPHI detector at LEP*, Eur. Phys. J. **C60** (2009) 17, arXiv:0901.4486.

[62] R. Essig, P. Schuster, N. Toro, and B. Wojtsekhowski, *An electron fixed target experiment to search for a new vector boson A' decaying to e^+e^-*, JHEP **02** (2011) 009, arXiv:1001.2557.

[63] M. Freytsis, G. Ovanesyan, and J. Thaler, *Dark force detection in low energy ep collisions*, JHEP **01** (2010) 111, arXiv:0909.2862.

[64] J. Balewski *et al.*, *DarkLight: A search for dark forces at the Jefferson Laboratory Free-Electron Laser Facility*, in *Proceedings, 2013 Community Summer Study on the Future of U.S. Particle Physics: Snowmass on the Mississippi (CSS2013): Minneapolis, MN, USA, July 29-August 6, 2013*, 2013, arXiv:1307.4432.

[65] B. Wojtsekhowski, D. Nikolenko, and I. Rachek, *Searching for a new force at VEPP-3*, arXiv:1207.5089.

[66] T. Beranek, H. Merkel, and M. Vanderhaeghen, *Theoretical framework to analyze searches for hidden light gauge bosons in electron scattering fixed target experiments*, Phys. Rev. **D88** (2013) 015032, arXiv:1303.2540.

[67] B. Echenard, R. Essig, and Y.-M. Zhong, *Projections for dark photon searches at Mu3e*, JHEP **01** (2015) 113, arXiv:1411.1770.

[68] M. Battaglieri *et al.*, *The Heavy Photon Search test detector*, Nucl. Instrum. Meth. **A777** (2015) 91, arXiv:1406.6115.

[69] M. Raggi and V. Kozhuharov, *Proposal to search for a dark photon in positron on target collisions at DAΦNE Linac*, Adv. High Energy Phys. **2014** (2014) 959802, arXiv:1403.3041.

[70] S. Alekhin *et al.*, *A facility to Search for Hidden Particles at the CERN SPS: the SHiP physics case*, Rept. Prog. Phys. **79** (2016) 124201, arXiv:1504.04855.

[71] S. Gardner, R. J. Holt, and A. S. Tadepalli, *New prospects in fixed target searches for dark forces with the SeaQuest experiment at Fermilab*, Phys. Rev. **D93** (2016) 115015, arXiv:1509.00050.

[72] P. Ilten, J. Thaler, M. Williams, and W. Xue, *Dark photons from charm mesons at LHCb*, Phys. Rev. **D92** (2015) 115017, arXiv:1509.06765.

[73] D. Curtin, R. Essig, S. Gori, and J. Shelton, *Illuminating dark photons with high-energy colliders*, JHEP **02** (2015) 157, arXiv:1412.0018.

[74] M. He, X.-G. He, and C.-K. Huang, *Dark photon search at a circular e^+e^- collider*, Int. J. Mod. Phys. **A32** (2017) 1750138, arXiv:1701.08614.

[75] J. Kozaczuk, *Dark photons from nuclear transitions*, Phys. Rev. **D97** (2018) 015014, arXiv:1708.06349.

[76] P. Ilten, Y. Soreq, J. Thaler, M. Williams, and W. Xue, *Proposed inclusive dark photon search at LHCb*, Phys. Rev. Lett. **116** (2016) 251803, arXiv:1603.08926.

[77] J. Alexander, *MMAPS: Missing-Mass A-Prime Search*, EPJ Web Conf. **142** (2017) 01001.

[78] M. He, X.-G. He, C.-K. Huang, and G. Li, *Search for a heavy dark photon at future e^+e^- colliders*, JHEP **03** (2018) 139, arXiv:1712.09095.

[79] J. L. Feng, I. Galon, F. Kling, and S. Trojanowski, *ForwArd Search ExpeRiment at the LHC*, Phys. Rev. **D97** (2018) 035001, arXiv:1708.09389.

[80] E. Nardi, C. D. R. Carvajal, A. Ghoshal, D. Meloni, and M. Raggi, *Resonant production of dark photons in positron beam dump experiments*, Phys. Rev. **D97** (2018) 095004, arXiv:1802.04756.

[81] M. D'Onofrio, O. Fischer, and Z. S. Wang, *Searching for dark photons at the LHeC and FCC-he*, arXiv:1909.02312.

[82] Y.-D. Tsai, P. deNiverville, and M. X. Liu, *The high-energy frontier of the intensity frontier: Closing the dark photon, inelastic dark matter, and muon g-2 windows*, arXiv:1908.07525.

[83] LHCb collaboration, R. Aaij *et al.*, *Search for dark photons produced in 13 TeV pp collisions*, Phys. Rev. Lett. **120** (2018) 061801, arXiv:1710.02867.

[84] S. Cassel, D. M. Ghilencea, and G. G. Ross, *Electroweak and dark matter constraints on a Z' in models with a hidden valley*, Nucl. Phys. **B827** (2010) 256, arXiv:0903.1118.

[85] J. M. Cline, G. Dupuis, Z. Liu, and W. Xue, *The windows for kinetically mixed Z'-mediated dark matter and the galactic center gamma ray excess*, JHEP **08** (2014) 131, arXiv:1405.7691.

[86] LHCb collaboration, A. A. Alves Jr. *et al.*, *The LHCb detector at the LHC*, JINST **3** (2008) S08005.

[87] LHCb collaboration, R. Aaij *et al.*, *LHCb detector performance*, Int. J. Mod. Phys. **A30** (2015) 1530022, arXiv:1412.6352.

[88] G. Dujany and B. Storaci, *Real-time alignment and calibration of the LHCb Detector in Run II*, J. Phys. Conf. Ser. **664** (2015) 082010.

[89] R. Aaij *et al.*, *Tesla: An application for real-time data analysis in high energy physics*, Comput. Phys. Commun. **208** (2016) 35, arXiv:1604.05596.

[90] T. Sjöstrand, S. Ask, J. R. Christiansen, R. Corke, N. Desai, P. Ilten, S. Mrenna, S. Prestel, C. O. Rasmussen, and P. Z. Skands, *An Introduction to PYTHIA 8.2*, Comput. Phys. Commun. **191** (2015) 159, arXiv:1410.3012; T. Sjöstrand, S. Mrenna, and P. Skands, *A brief introduction to PYTHIA 8.1*, Comput. Phys. Commun. **178** (2008) 852, arXiv:0710.3820.

[91] I. Belyaev *et al.*, *Handling of the generation of primary events in Gauss, the LHCb simulation framework*, J. Phys. Conf. Ser. **331** (2011) 032047.

[92] Geant4 collaboration, J. Allison, K. Amako, J. Apostolakis, H. Araujo, P. A. Dubois *et al.*, *Geant4 developments and applications*, IEEE Trans. Nucl. Sci. **53** (2006) 270; Geant4 collaboration, S. Agostinelli *et al.*, *Geant4: A simulation toolkit*, Nucl. Instrum. Meth. **A506** (2003) 250.

[93] R. Aaij *et al.*, *The LHCb trigger and its performance in 2011*, JINST **8** (2013) P04022, arXiv:1211.3055.

[94] M. Cacciari, G. P. Salam, and G. Soyez, *The anti-k_T jet clustering algorithm*, JHEP **0804** (2008) 063, arXiv:0802.1189.

[95] M. Cacciari, G. P. Salam, and G. Soyez, *FastJet user manual*, Eur. Phys. J. **C72** (2012) 1896, arXiv:1111.6097.

[96] LHCb collaboration, R. Aaij *et al.*, *Study of forward Z +jet production in* pp *collisions at* $\sqrt{s} = 7\,TeV$, JHEP **01** (2014) 033, arXiv:1310.8197.

[97] See the Supplemental Material to this Letter for additional fit details and figures.

[98] M. Williams, *A novel approach to the bias-variance problem in bump hunting*, JINST **12** (2017) P09034, arXiv:1705.03578.

[99] P. D. Dauncey, M. Kenzie, N. Wardle, and G. J. Davies, *Handling uncertainties in background shapes*, JINST **10** (2015) P04015, arXiv:1408.6865.

[100] P. Ilten, Y. Soreq, M. Williams, and W. Xue, *Serendipity in dark photon searches*, JHEP **06** (2018) 004, arXiv:1801.04847.

[101] P. Fayet, *Extra U(1)'s and new forces*, Nucl. Phys. **B347** (1990) 743.

[102] CMS collaboration, *Search for a narrow resonance decaying to a pair of muons in proton-proton collisions at 13 TeV*, Tech. Rep. CMS-PAS-EXO-19-018, CERN, Geneva, 2019.

[103] R. Aaij *et al.*, *Performance of the LHCb Vertex Locator*, JINST **9** (2014) P09007, arXiv:1405.7808.

[104] M. Alexander *et al.*, *Mapping the material in the LHCb vertex locator using secondary hadronic interactions*, JINST **13** (2018) P06008, arXiv:1803.07466.

[105] T. Likhomanenko, P. Ilten, E. Khairullin, A. Rogozhnikov, A. Ustyuzhanin, and M. Williams, *LHCb topological trigger reoptimization*, J. Phys. Conf. Ser. **664** (2015) 082025, arXiv:1510.00572.

[106] V. V. Gligorov and M. Williams, *Efficient, reliable and fast high-level triggering using a bonsai boosted decision tree*, JINST **8** (2013) P02013, arXiv:1210.6861.

[107] LHCb collaboration, R. Aaij *et al.*, *Measurement of the* $B_s^0 \to \mu^+\mu^-$ *branching fraction and effective lifetime and search for* $B^0 \to \mu^+\mu^-$ *decays*, Phys. Rev. Lett. **118** (2017) 191801, arXiv:1703.05747.

Supplemental Material for LHCb-PAPER-2019-031

Search for $A' \to \mu^+\mu^-$ decays

Additional details and figures for the prompt-like and long-lived searches are presented in this Supplemental Material.

Isolation Criterion

For masses above the $\phi(1020)$ meson mass, dark photons are expected to be predominantly produced in Drell–Yan processes in pp collisions at the LHC. A well-known signature of Drell–Yan production is dimuon pairs that are largely isolated, and a high-mass dark photon would inherit this property. The signal sensitivity for $m(A') > 1.1\,\text{GeV}$ is enhanced by applying the jet-based isolation requirement used in Ref. [83]. Jet reconstruction is performed by clustering charged and neutral particle-flow candidates [96] using the anti-k_{T} clustering algorithm [94] with $R = 0.5$ as implemented in FastJet [95]. Muons with $p_{\text{T}}(\mu)/p_{\text{T}}(\text{jet}) < 0.7$ are rejected, where the contribution to $p_{\text{T}}(\text{jet})$ from the other muon is excluded if both muons are clustered in the same jet, as this is found to provide nearly optimal sensitivity for all $m(A') > m(\phi)$.

Prompt-Like Fits

The prompt-like fit strategy is the same as described in detail in the Supplemental Material of Ref. [83]. This strategy was first introduced in Ref. [98], where it is denoted by aic-o. The $m(\mu^+\mu^-)$ spectrum is scanned in steps of $\sigma[m(\mu^+\mu^-)]/2$ searching for $A' \to \mu^+\mu^-$ contributions. At each mass, a binned extended maximum likelihood fit is performed, and the profile likelihood is used to determine the p-value and the confidence interval on $n_{\text{ob}}^{A'}[m(A')]$. The prompt-like-search trials factor is obtained using pseudoexperiments. As in Ref. [98], each fit is performed in a $\pm 12.5\,\sigma[m(\mu^+\mu^-)]$ window around the scan-mass value using bins with widths of $\sigma[m(\mu^+\mu^-)]/20$. Near threshold, the energy released in the decay, $\sqrt{m(\mu^+\mu^-)^2 - 4m(\mu)^2}$, is used instead of the mass since it is easier to model. The confidence intervals are defined using the *bounded likelihood* approach, which involves taking $\Delta \log \mathcal{L}$ relative to zero signal, rather than the best-fit value, if the best-fit signal value is negative. This approach enforces that only physical (nonnegative) upper limits are placed on $n_{\text{ob}}^{A'}[m(A')]$, and prevents defining exclusion regions that are much better than the experimental sensitivity in cases where a large deficit in the background yield is observed.

The signal models are determined at each $m(A')$ using a combination of simulated $A' \to \mu^+\mu^-$ decays and the widths of the large resonance peaks that are clearly visible in the data. The background models take as input a large set of potential background components, then the data-driven model-selection process of Ref. [98] is performed, whose uncertainty is included in the profile likelihood following Ref. [99]. Specifically, the method labeled *aic-o* in Ref. [98] is used, where the log-likelihood of each background model is penalized for its complexity (number of parameters). The confidence intervals are obtained from the profile likelihoods, including the penalty terms, where the model index is treated as a discrete nuisance parameter, as originally proposed in Ref. [99]. In this analysis, the set of possible background components includes all Legendre modes with $\ell \leq 10$ at every $m(A')$. Additionally, dedicated background components are included for sizable narrow SM resonance contributions. The use of 11 Legendre modes adequately describes

every double-misidentified peaking background that contributes at a significant level, and therefore, these do not require dedicated background components. In mass regions where such complexity is not required, the data-driven model-selection procedure reduces the complexity which increases the sensitivity to a potential signal contribution. Therefore, the impact of the background-model uncertainty on the size of the confidence intervals is mass dependent, though on average it is about 30%. As in Ref. [98], all fit regions are transformed onto the interval $[-1, 1]$, where the scan $m(A')$ value maps to zero. After such a transformation, the signal model is (approximately) an even function; therefore, odd Legendre modes are orthogonal to the signal component, which means that the presence of odd modes has minimal impact on the variance of $n_{\rm ob}^{A'}[m(A')]$. In the prompt-like fits, all odd Legendre modes up to ninth order are included in every background model, while only a subset of the even modes is selected for inclusion in each fit.

Regions in the mass spectrum where large known resonance contributions are observed are vetoed in the prompt-like A' search. Furthermore, the regions near the η' meson and the excited Υ states (beyond the $\Upsilon(3S)$ meson) are treated specially. For example, since it is not possible to distinguish between $A' \to \mu^+\mu^-$ and $\eta' \to \mu^+\mu^-$ contributions at $m(\eta')$, the p-values near this mass are ignored. The small excess at $m(\eta')$ is treated as signal when setting the limits on $n_{\rm ob}^{A'}[m(A')]$, which is conservative in that an $\eta' \to \mu^+\mu^-$ contribution will weaken the constraints on $A' \to \mu^+\mu^-$ decays. The same strategy is used near the excited Υ masses.

Long-Lived Fits

The long-lived fit strategy is also the same as described in the Supplemental Material to Ref. [83]. The signal yields are determined from binned extended maximum likelihood fits performed on all long-lived $A' \to \mu^+\mu^-$ candidates using the three-dimensional feature space of $m(\mu^+\mu^-)$, t, and $\chi^2_{\rm DF}$. As in the prompt-like A' search, a scan is performed in discrete steps of $\sigma[m(\mu^+\mu^-)]/2$; however, in this case, discrete steps in $\tau(A')$ are also considered. The profile likelihood is again used to obtain the p-values and the confidence intervals on $n_{\rm ob}^{A'}[m(A'), \tau(A')]$. The binning scheme involves four bins in $\chi^2_{\rm DF}$: [0,2], [2,4], [4,6], and [6,8]. Eight bins in t are used: [0.2,0.6], [0.6,1.1], [1.1,1.6], [1.6,2.2], [2.2,3.0], [3,5], [5,10], and $> 10\,$ps. The binning scheme used for $m(\mu^+\mu^-)$ depends on the scan $m(A')$ value, and is chosen such that the vast majority of the signal falls into a single bin. Signal decays mostly have small $\chi^2_{\rm DF}$ values, with about 50% (80%) of $A' \to \mu^+\mu^-$ decays satisfying $\chi^2_{\rm DF} < 2\,(4)$. Background from b-hadron decays populates the small t region and is roughly uniformly distributed in $\chi^2_{\rm DF}$, whereas background from $K^0_{\rm S}$ decays is signal-like in $\chi^2_{\rm DF}$ and roughly uniformly distributed in t. Figure S5 shows the three-dimensional distribution of all long-lived $A' \to \mu^+\mu^-$ candidates.

The expected contribution in each bin from photon conversions is derived from the number of candidates rejected by the conversion criterion. Two large control data samples are used to develop and validate the modeling of the b-hadron and $K^0_{\rm S}$ contributions. Both contributions are well modeled by second-order polynomials in $\sqrt{m(\mu^+\mu^-)^2 - 4m(\mu)^2}$. While no evidence for t or $\chi^2_{\rm DF}$ dependence is observed for these parameters in either the b-hadron or $K^0_{\rm S}$ control sample, all parameters are allowed to vary independently in each $[t, \chi^2_{\rm DF}]$ region in the fits used in the long-lived A' search.

Figure S6 shows the long-lived $A' \to \mu^+\mu^-$ candidates, along with the pull values obtained from fits performed to the data where no signal contributions are included. These

distributions are consistent with those observed in pseudoexperiments where no signal component is generated. Specifically, the data are consistent with being predominantly due to b-hadron decays at small t, and due to K^0_S decays for large t and $m(\mu^+\mu^-) \gtrsim 280\,\text{MeV}$. The remaining few candidates at large t and small $m(\mu^+\mu^-)$ are likely photon conversions. *N.b.*, the same dominant backgrounds are expected in the upgraded LHCb detector in each region of mass and decay time.

Long-Lived Efficiency Determination

The value of $\epsilon^{A'}_{\gamma^*}[m(A'), \tau(A')]$ is not unity in the long-lived A' search, in part because the efficiency depends on the decay time, t. The kinematics are identical for $A' \to \mu^+\mu^-$ and prompt $\gamma^* \to \mu^+\mu^-$ decays for $m(A') = m(\gamma^*)$; therefore, the t dependence of $\epsilon^{A'}_{\gamma^*}[m(A'), \tau(A')]$ is obtained by resampling prompt $\gamma^* \to \mu^+\mu^-$ candidates as long-lived $A' \to \mu^+\mu^-$ decays, where all t-dependent properties, *e.g.* $\min[\chi^2_{\text{IP}}(\mu^\pm)]$, are recalculated based on the resampled decay-vertex locations. The impact of background contamination in the prompt $\gamma^* \to \mu^+\mu^-$ sample is shown to be negligible by recomputing $\epsilon^{A'}_{\gamma^*}[m(A'), \tau(A')]$ using same-sign $\mu^\pm\mu^\pm$ candidates, which are purely background, instead of prompt $\gamma^* \to \mu^+\mu^-$ candidates in this procedure. The high-precision three-dimensional material map produced from a data sample of secondary hadronic interactions in Ref. [104], which forms the basis of the photon-conversion criterion applied in the selection, is used here to determine where each muon would hit active sensors, and thus, have recorded hits in the VELO. The resolution on the vertex location and other t-dependent properties varies strongly with the location of the first VELO hit on each muon track, though this dependence is largely geometric, making rescaling the resolution of prompt tracks straightforward. Finally, the values used for the decay-fit χ^2_{DF} are resampled from the observed distribution for K^0_S decays in data, which is similar to that expected for an ideal χ^2 distribution with three degrees of freedom, to ensure that non-Gaussian effects are properly considered.

This approach is validated using simulation, where prompt $A' \to \mu^+\mu^-$ decays are used to predict the properties of long-lived $A' \to \mu^+\mu^-$ decays. Figure S1 shows one such example using A' decays generated with zero lifetime to predict the radial flight distance of a sample produced with $\tau(A') = 2\,\text{ps}$. Here, the full long-lived selection is applied except for the photon-conversion criterion, which is validated separately as discussed below. Since this validation study involves only simulated decays, the material map produced in Ref. [104] is replaced by the geometry used in the simulation. The integrated long-lived $A' \to \mu^+\mu^-$ yield predictions agree to $\approx 2\%$ with the actual values in the $[m(A'), \tau(A')]$ region explored in the long-lived A' search. Both the short-distance turn-on (driven by the $\min[\chi^2_{\text{IP}}(\mu^\pm)]$ criterion) and long-distance turn-off (driven by the minimum number of VELO hits required to form a track) curves are well described. The dominant uncertainty here arises due to limited knowledge of how radiation damage has affected the performance of the VELO as a function of the distance from the pp interaction region. This uncertainty is estimated to be 5% by rerunning the resampling method many times under different radiation-damage hypotheses.

To validate the efficiency of the photon-conversion criterion, the predicted efficiency for a dark photon with the same mass and lifetime as the K^0_S meson is compared to the efficiency observed in a control data sample of K^0_S decays. The predicted and observed efficiencies agree to 1%. Additionally, in Ref. [104] the expected performance of the

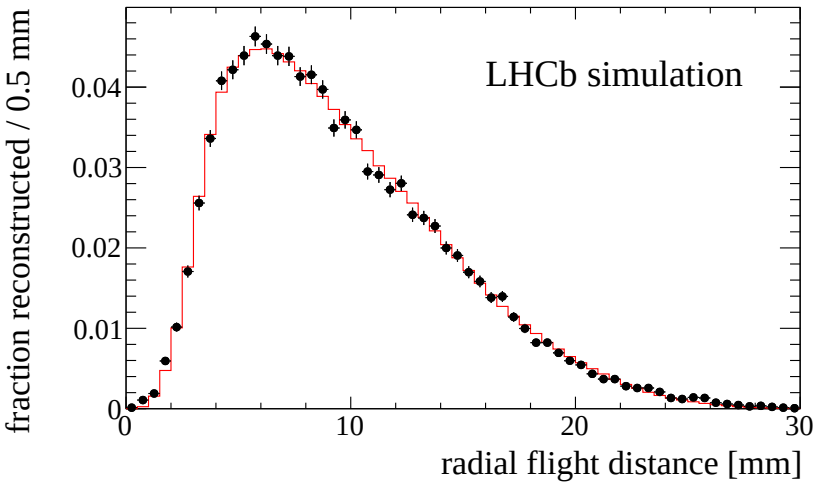

Figure S1: Validation of the data-driven approach used to predict the long-lived A' properties from prompt $\gamma^* \to \mu^+\mu^-$ candidates in data is shown using two simulated $A' \to \mu^+\mu^-$ samples, each generated with the same production kinematics, for (black points) $\tau(A') = 2\,\text{ps}$ reconstructed and satisfying the long-lived selection criteria except the photon-conversion criterion, and (red line) the prediction for $\tau(A') = 2\,\text{ps}$ based only on the prompt $A' \to \mu^+\mu^-$ sample. *N.b.*, there is no free normalization factor, the red yield is predicted entirely from the prompt sample.

photon-conversion criterion was shown to agree with the performance observed in an independent control data sample of photon conversions out to the $\mathcal{O}(10^{-4})$ level. The expected performance here was obtained in a similar manner to how the dark photon efficiencies are obtained, except starting from a pure sample of conversions instead of prompt $\gamma^* \to \mu^+\mu^-$ candidates.

The looser kinematic, muon-identification, and hardware-trigger requirements applied to long-lived $A' \to \mu^+\mu^-$ candidates, *cf.* prompt-like candidates, also increase the efficiency. This t-independent increase in efficiency is determined using a control data sample of dimuon candidates consistent with originating from the PV, but otherwise satisfying the long-lived criteria. Specifically, $\min[\chi^2_{\text{IP}}(\mu^\pm)]$ fits like those used to determine $n^{\gamma^*}_{\text{ob}}[m(A')]$ in the prompt-like A' search are run on this control sample and on the subset of its candidates that satisfy the more stringent criteria applied in the prompt-like A' search. The decrease in the $\gamma^* \to \mu^+\mu^-$ yield observed when applying the more stringent criteria at each mass is used to determine the t-independent increase in efficiency.

Additional Figures

This section provides additional figures from the analysis, and more detailed comparisons of the new constraints presented in the Letter with previous results.

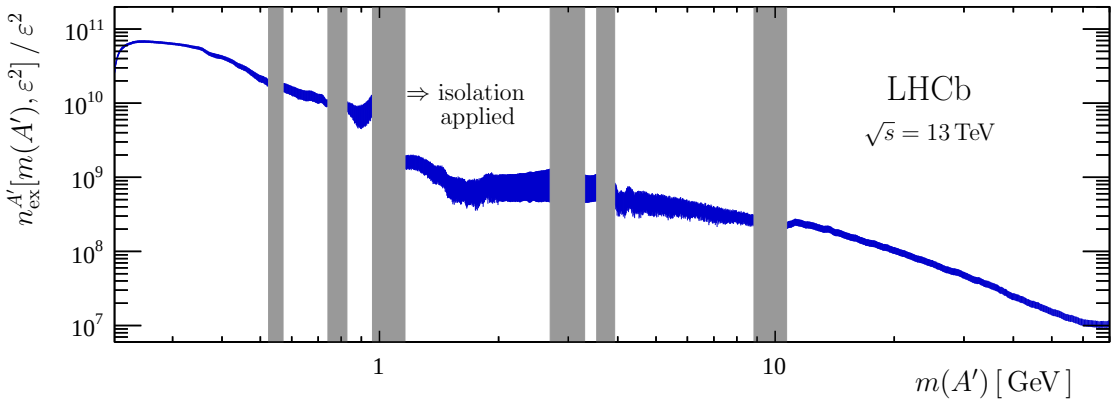

Figure S2: Expected reconstructed and selected prompt-like $A' \to \mu^+\mu^-$ yield divided by ε^2, where the displayed uncertainties include the systematic contributions. The gray boxes cover the regions with large SM resonance contributions, where no search for dark photons is performed. The anti-$k_{\rm T}$-based isolation requirement is applied for $m(A') > 1.1\,\text{GeV}$.

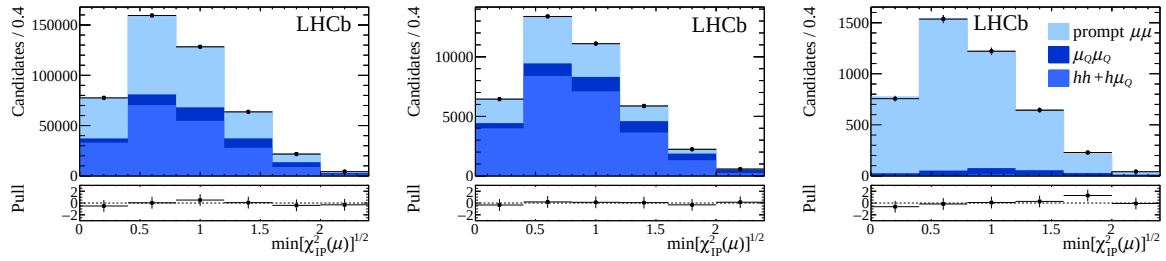

Figure S3: Example $\min[\chi^2_{\rm IP}(\mu^\pm)]^{1/2}$ distributions with fit results overlaid for prompt-like candidates near (left) $m(A') = 0.5$, (middle) 5, and (right) 50 GeV. The square root of $\min[\chi^2_{\rm IP}(\mu^\pm)]$ is used in the fits to increase the bin occupancies at large $\min[\chi^2_{\rm IP}(\mu^\pm)]$ values. The background categories, as described in the Letter, are as follows: (hh) two prompt hadrons misidentified as muons; $(h\mu_Q)$ a misidentified prompt hadron combined with a muon produced in the decay of a heavy-flavor quark, Q, that is misidentified as prompt; and $(\mu_Q\mu_Q)$ two muons produced in Q-hadron decays that are both misidentified as prompt.

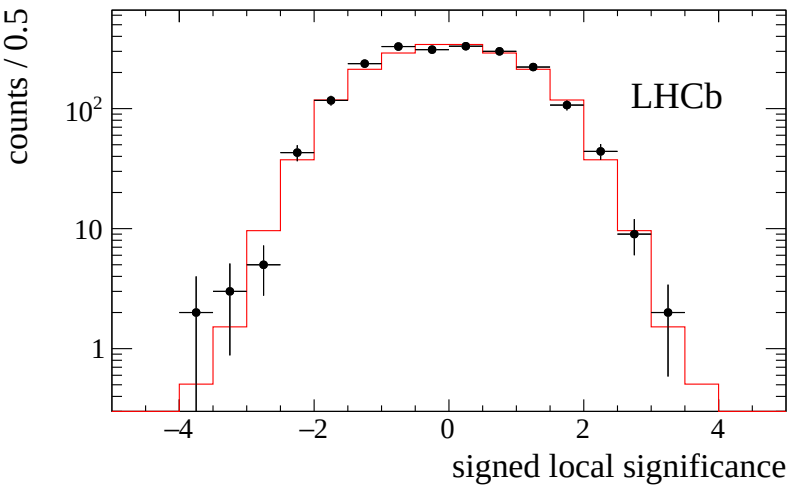

Figure S4: Signed local significances at each scan mass from (black points) all fits and (red) the expected distribution; if the best-fit signal-yield estimator is negative, the signed significance is negative and *vice versa*. The error bars account for the correlation between nearest-neighbor fit results, which often produces outliers in pairs due to the $\sigma[m(\mu^+\mu^-)]/2$ step size.

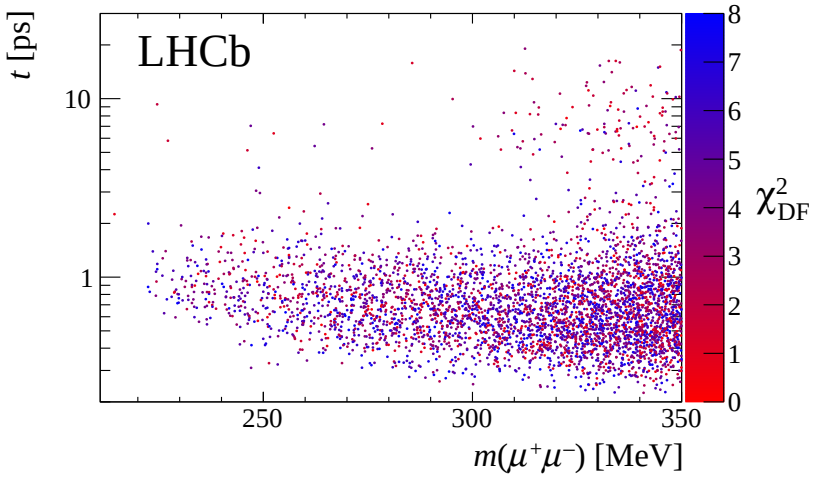

Figure S5: Three-dimensional distribution of $\chi^2_{\rm DF}$ versus t versus $m(\mu^+\mu^-)$, which is fit to determine the long-lived signal yields. The data are consistent with being predominantly due to b-hadron decays at small t, and due to $K^0_{\rm S}$ decays for large t and $m(\mu^+\mu^-) \gtrsim 280\,\text{MeV}$. The remaining few candidates at large t and small $m(\mu^+\mu^-)$ are likely photon conversions.

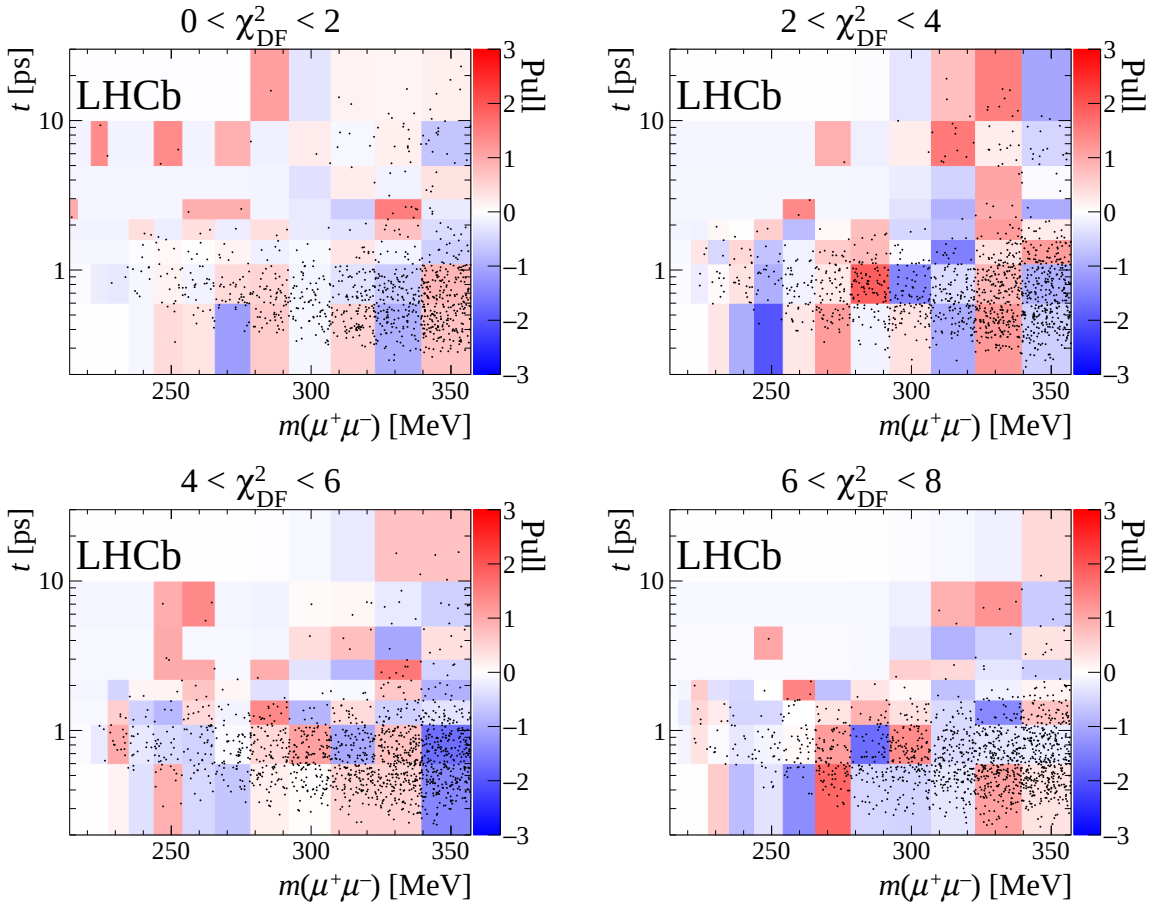

Figure S6: Long-lived $A' \to \mu^+\mu^-$ candidates (black points) showing t versus $m(\mu^+\mu^-)$ in bins of $\chi^2_{\rm DF}$, compared to the pulls from binned fits performed without a signal contribution (color axis). Positive pulls denote an excess of data candidates.

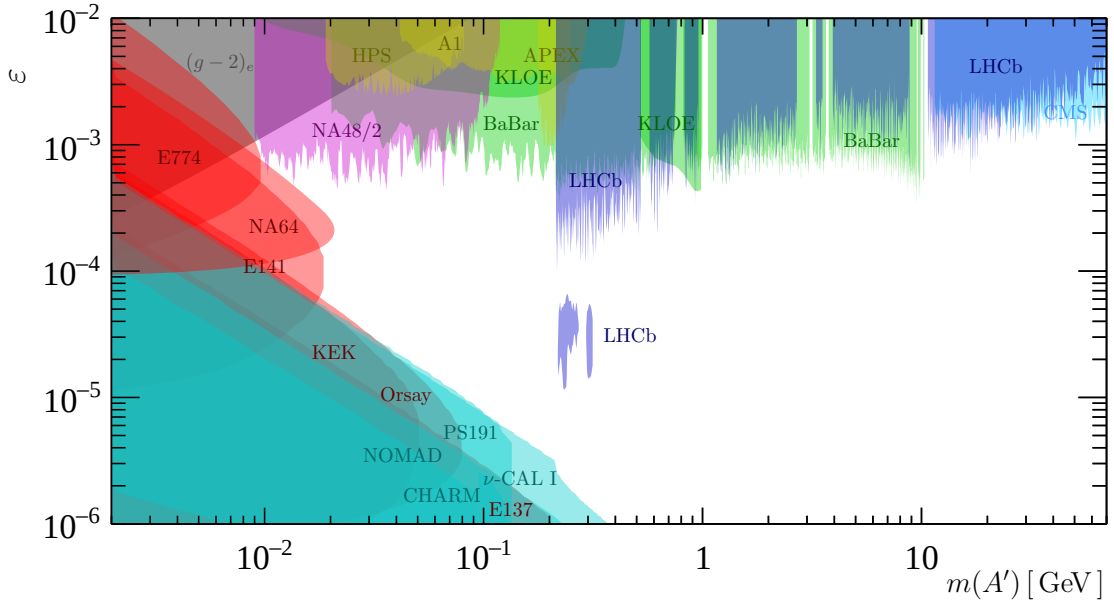

Figure S7: Comparison of the results presented in this Letter to existing constraints from previous experiments in the few-loop ε region (see Ref. [100] for details about previous experiments).

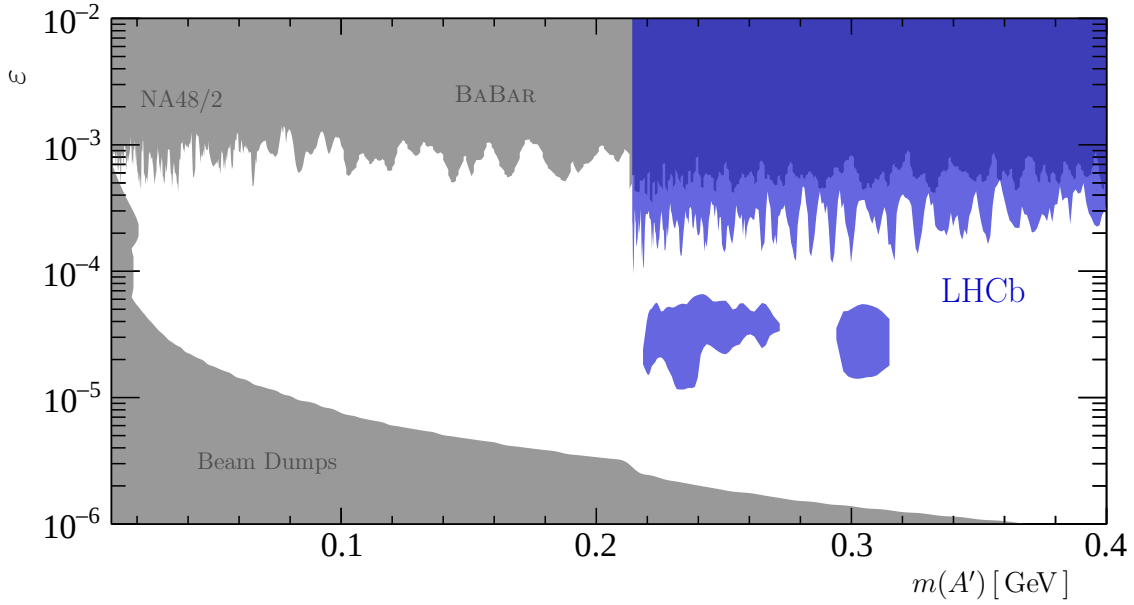

Figure S8: Comparison of the results presented in this Letter to existing constraints from previous experiments in the few-loop ε region (see Ref. [100] for details about previous experiments), restricted to the mass region motivated by self-interacting dark matter [4].

LHCb collaboration

R. Aaij[31], C. Abellán Beteta[49], T. Ackernley[59], B. Adeva[45], M. Adinolfi[53], H. Afsharnia[9], C.A. Aidala[79], S. Aiola[25], Z. Ajaltouni[9], S. Akar[64], P. Albicocco[22], J. Albrecht[14], F. Alessio[47], M. Alexander[58], A. Alfonso Albero[44], G. Alkhazov[37], P. Alvarez Cartelle[60], A.A. Alves Jr[45], S. Amato[2], Y. Amhis[11], L. An[21], L. Anderlini[21], G. Andreassi[48], M. Andreotti[20], F. Archilli[16], J. Arnau Romeu[10], A. Artamonov[43], M. Artuso[67], K. Arzymatov[41], E. Aslanides[10], M. Atzeni[49], B. Audurier[26], S. Bachmann[16], J.J. Back[55], S. Baker[60], V. Balagura[11,b], W. Baldini[20,47], A. Baranov[41], R.J. Barlow[61], S. Barsuk[11], W. Barter[60], M. Bartolini[23,47,h], F. Baryshnikov[76], G. Bassi[28], V. Batozskaya[35], B. Batsukh[67], A. Battig[14], V. Battista[48], A. Bay[48], M. Becker[14], F. Bedeschi[28], I. Bediaga[1], A. Beiter[67], L.J. Bel[31], V. Belavin[41], S. Belin[26], N. Beliy[5], V. Bellee[48], K. Belous[43], I. Belyaev[38], G. Bencivenni[22], E. Ben-Haim[12], S. Benson[31], S. Beranek[13], A. Berezhnoy[39], R. Bernet[49], D. Berninghoff[16], H.C. Bernstein[67], E. Bertholet[12], A. Bertolin[27], C. Betancourt[49], F. Betti[19,e], M.O. Bettler[54], Ia. Bezshyiko[49], S. Bhasin[53], J. Bhom[33], M.S. Bieker[14], S. Bifani[52], P. Billoir[12], A. Bizzeti[21,u], M. Bjørn[62], M.P. Blago[47], T. Blake[55], F. Blanc[48], S. Blusk[67], D. Bobulska[58], V. Bocci[30], O. Boente Garcia[45], T. Boettcher[63], A. Boldyrev[77], A. Bondar[42,x], N. Bondar[37], S. Borghi[61,47], M. Borisyak[41], M. Borsato[16], J.T. Borsuk[33], T.J.V. Bowcock[59], C. Bozzi[20], S. Braun[16], A. Brea Rodriguez[45], M. Brodski[47], J. Brodzicka[33], A. Brossa Gonzalo[55], D. Brundu[26], E. Buchanan[53], A. Buonaura[49], C. Burr[47], A. Bursche[26], J.S. Butter[31], J. Buytaert[47], W. Byczynski[47], S. Cadeddu[26], H. Cai[71], R. Calabrese[20,g], L. Calero Diaz[22], S. Cali[22], R. Calladine[52], M. Calvi[24,i], M. Calvo Gomez[44,m], A. Camboni[44], P. Campana[22], D.H. Campora Perez[47], L. Capriotti[19,e], A. Carbone[19,e], G. Carboni[29], R. Cardinale[23,h], A. Cardini[26], P. Carniti[24,i], K. Carvalho Akiba[31], A. Casais Vidal[45], G. Casse[59], M. Cattaneo[47], G. Cavallero[47], R. Cenci[28,p], J. Cerasoli[10], M.G. Chapman[53], M. Charles[12,47], Ph. Charpentier[47], G. Chatzikonstantinidis[52], M. Chefdeville[8], V. Chekalina[41], C. Chen[3], S. Chen[26], A. Chernov[33], S.-G. Chitic[47], V. Chobanova[45], M. Chrzaszcz[47], A. Chubykin[37], P. Ciambrone[22], M.F. Cicala[55], X. Cid Vidal[45], G. Ciezarek[47], F. Cindolo[19], P.E.L. Clarke[57], M. Clemencic[47], H.V. Cliff[54], J. Closier[47], J.L. Cobbledick[61], V. Coco[47], J.A.B. Coelho[11], J. Cogan[10], E. Cogneras[9], L. Cojocariu[36], P. Collins[47], T. Colombo[47], A. Comerma-Montells[16], A. Contu[26], N. Cooke[52], G. Coombs[58], S. Coquereau[44], G. Corti[47], C.M. Costa Sobral[55], B. Couturier[47], D.C. Craik[63], J. Crkovska[66], A. Crocombe[55], M. Cruz Torres[1], R. Currie[57], C.L. Da Silva[66], E. Dall'Occo[31], J. Dalseno[45,53], C. D'Ambrosio[47], A. Danilina[38], P. d'Argent[16], A. Davis[61], O. De Aguiar Francisco[47], K. De Bruyn[47], S. De Capua[61], M. De Cian[48], J.M. De Miranda[1], L. De Paula[2], M. De Serio[18,d], P. De Simone[22], J.A. de Vries[31], C.T. Dean[66], W. Dean[79], D. Decamp[8], L. Del Buono[12], B. Delaney[54], H.-P. Dembinski[15], M. Demmer[14], A. Dendek[34], V. Denysenko[49], D. Derkach[77], O. Deschamps[9], F. Desse[11], F. Dettori[26], B. Dey[7], A. Di Canto[47], P. Di Nezza[22], S. Didenko[76], H. Dijkstra[47], F. Dordei[26], M. Dorigo[28,y], A.C. dos Reis[1], L. Douglas[58], A. Dovbnya[50], K. Dreimanis[59], M.W. Dudek[33], L. Dufour[47], G. Dujany[12], P. Durante[47], J.M. Durham[66], D. Dutta[61], R. Dzhelyadin[43,†], M. Dziewiecki[16], A. Dziurda[33], A. Dzyuba[37], S. Easo[56], U. Egede[60], V. Egorychev[38], S. Eidelman[42,x], S. Eisenhardt[57], R. Ekelhof[14], S. Ek-In[48], L. Eklund[58], S. Ely[67], A. Ene[36], S. Escher[13], S. Esen[31], T. Evans[47], A. Falabella[19], J. Fan[3], N. Farley[52], S. Farry[59], D. Fazzini[11], M. Féo[47], P. Fernandez Declara[47], A. Fernandez Prieto[45], F. Ferrari[19,e], L. Ferreira Lopes[48], F. Ferreira Rodrigues[2], S. Ferreres Sole[31], M. Ferrillo[49], M. Ferro-Luzzi[47], S. Filippov[40], R.A. Fini[18], M. Fiorini[20,g], M. Firlej[34], K.M. Fischer[62], C. Fitzpatrick[47], T. Fiutowski[34], F. Fleuret[11,b], M. Fontana[47], F. Fontanelli[23,h], R. Forty[47], V. Franco Lima[59], M. Franco Sevilla[65], M. Frank[47], C. Frei[47], D.A. Friday[58], J. Fu[25,q], M. Fuehring[14], W. Funk[47], E. Gabriel[57], A. Gallas Torreira[45], D. Galli[19,e], S. Gallorini[27], S. Gambetta[57], Y. Gan[3], M. Gandelman[2], P. Gandini[25], Y. Gao[4], L.M. Garcia Martin[46], J. García Pardiñas[49],

B. Garcia Plana[45], F.A. Garcia Rosales[11], J. Garra Tico[54], L. Garrido[44], D. Gascon[44], C. Gaspar[47], D. Gerick[16], E. Gersabeck[61], M. Gersabeck[61], T. Gershon[55], D. Gerstel[10], Ph. Ghez[8], V. Gibson[54], A. Gioventù[45], O.G. Girard[48], P. Gironella Gironell[44], L. Giubega[36], C. Giugliano[20], K. Gizdov[57], V.V. Gligorov[12], C. Göbel[69], D. Golubkov[38], A. Golutvin[60,76], A. Gomes[1,a], P. Gorbounov[38,6], I.V. Gorelov[39], C. Gotti[24,i], E. Govorkova[31], J.P. Grabowski[16], R. Graciani Diaz[44], T. Grammatico[12], L.A. Granado Cardoso[47], E. Graugés[44], E. Graverini[48], G. Graziani[21], A. Grecu[36], R. Greim[31], P. Griffith[20], L. Grillo[61], L. Gruber[47], B.R. Gruberg Cazon[62], C. Gu[3], E. Gushchin[40], A. Guth[13], Yu. Guz[43,47], T. Gys[47], T. Hadavizadeh[62], G. Haefeli[48], C. Haen[47], S.C. Haines[54], P.M. Hamilton[65], Q. Han[7], X. Han[16], T.H. Hancock[62], S. Hansmann-Menzemer[16], N. Harnew[62], T. Harrison[59], R. Hart[31], C. Hasse[47], M. Hatch[47], J. He[5], M. Hecker[60], K. Heijhoff[31], K. Heinicke[14], A. Heister[14], A.M. Hennequin[47], K. Hennessy[59], L. Henry[46], J. Heuel[13], A. Hicheur[68], R. Hidalgo Charman[61], D. Hill[62], M. Hilton[61], P.H. Hopchev[48], J. Hu[16], W. Hu[7], W. Huang[5], W. Hulsbergen[31], T. Humair[60], R.J. Hunter[55], M. Hushchyn[77], D. Hutchcroft[59], D. Hynds[31], P. Ibis[14], M. Idzik[34], P. Ilten[52], A. Inglessi[37], A. Inyakin[43], K. Ivshin[37], R. Jacobsson[47], S. Jakobsen[47], J. Jalocha[62], E. Jans[31], B.K. Jashal[46], A. Jawahery[65], V. Jevtic[14], F. Jiang[3], M. John[62], D. Johnson[47], C.R. Jones[54], B. Jost[47], N. Jurik[62], S. Kandybei[50], M. Karacson[47], J.M. Kariuki[53], N. Kazeev[77], M. Kecke[16], F. Keizer[54], M. Kelsey[67], M. Kenzie[54], T. Ketel[32], B. Khanji[47], A. Kharisova[78], K.E. Kim[67], T. Kirn[13], V.S. Kirsebom[48], S. Klaver[22], K. Klimaszewski[35], S. Koliiev[51], A. Kondybayeva[76], A. Konoplyannikov[38], P. Kopciewicz[34], R. Kopecna[16], P. Koppenburg[31], I. Kostiuk[31,51], O. Kot[51], S. Kotriakhova[37], L. Kravchuk[40], R.D. Krawczyk[47], M. Kreps[55], F. Kress[60], S. Kretzschmar[13], P. Krokovny[42,x], W. Krupa[34], W. Krzemien[35], W. Kucewicz[33,l], M. Kucharczyk[33], V. Kudryavtsev[42,x], H.S. Kuindersma[31], G.J. Kunde[66], A.K. Kuonen[48], T. Kvaratskheliya[38], D. Lacarrere[47], G. Lafferty[61], A. Lai[26], D. Lancierini[49], J.J. Lane[61], G. Lanfranchi[22], C. Langenbruch[13], T. Latham[55], F. Lazzari[28,v], C. Lazzeroni[52], R. Le Gac[10], R. Lefèvre[9], A. Leflat[39], F. Lemaitre[47], O. Leroy[10], T. Lesiak[33], B. Leverington[16], H. Li[70], X. Li[66], Y. Li[6], Z. Li[67], X. Liang[67], R. Lindner[47], F. Lionetto[49], V. Lisovskyi[11], G. Liu[70], X. Liu[3], D. Loh[55], A. Loi[26], J. Lomba Castro[45], I. Longstaff[58], J.H. Lopes[2], G. Loustau[49], G.H. Lovell[54], Y. Lu[6], D. Lucchesi[27,o], M. Lucio Martinez[31], Y. Luo[3], A. Lupato[27], E. Luppi[20,g], O. Lupton[55], A. Lusiani[28], X. Lyu[5], S. Maccolini[19,e], F. Machefert[11], F. Maciuc[36], V. Macko[48], P. Mackowiak[14], S. Maddrell-Mander[53], L.R. Madhan Mohan[53], O. Maev[37,47], A. Maevskiy[77], K. Maguire[61], D. Maisuzenko[37], M.W. Majewski[34], S. Malde[62], B. Malecki[47], A. Malinin[75], T. Maltsev[42,x], H. Malygina[16], G. Manca[26,f], G. Mancinelli[10], R. Manera Escalero[44], D. Manuzzi[19,e], D. Marangotto[25,q], J. Maratas[9,w], J.F. Marchand[8], U. Marconi[19], S. Mariani[21], C. Marin Benito[11], M. Marinangeli[48], P. Marino[48], J. Marks[16], P.J. Marshall[59], G. Martellotti[30], L. Martinazzoli[47], M. Martinelli[24], D. Martinez Santos[45], F. Martinez Vidal[46], A. Massafferri[1], M. Materok[13], R. Matev[47], A. Mathad[49], Z. Mathe[47], V. Matiunin[38], C. Matteuzzi[24], K.R. Mattioli[79], A. Mauri[49], E. Maurice[11,b], M. McCann[60,47], L. Mcconnell[17], A. McNab[61], R. McNulty[17], J.V. Mead[59], B. Meadows[64], C. Meaux[10], G. Meier[14], N. Meinert[73], D. Melnychuk[35], S. Meloni[24,i], M. Merk[31], A. Merli[25], M. Mikhasenko[47], D.A. Milanes[72], E. Millard[55], M.-N. Minard[8], O. Mineev[38], L. Minzoni[20,g], S.E. Mitchell[57], B. Mitreska[61], D.S. Mitzel[47], A. Mödden[14], A. Mogini[12], R.D. Moise[60], T. Mombächer[14], I.A. Monroy[72], S. Monteil[9], M. Morandin[27], G. Morello[22], M.J. Morello[28,t], J. Moron[34], A.B. Morris[10], A.G. Morris[55], R. Mountain[67], H. Mu[3], F. Muheim[57], M. Mukherjee[7], M. Mulder[31], D. Müller[47], K. Müller[49], V. Müller[14], C.H. Murphy[62], D. Murray[61], P. Muzzetto[26], P. Naik[53], T. Nakada[48], R. Nandakumar[56], A. Nandi[62], T. Nanut[48], I. Nasteva[2], M. Needham[57], N. Neri[25,q], S. Neubert[16], N. Neufeld[47], R. Newcombe[60], T.D. Nguyen[48], C. Nguyen-Mau[48,n], E.M. Niel[11], S. Nieswand[13], N. Nikitin[39], N.S. Nolte[47], C. Nunez[79], A. Oblakowska-Mucha[34], V. Obraztsov[43], S. Ogilvy[58], D.P. O'Hanlon[19], R. Oldeman[26,f], C.J.G. Onderwater[74], J. D. Osborn[79], A. Ossowska[33], J.M. Otalora Goicochea[2], T. Ovsiannikova[38], P. Owen[49], A. Oyanguren[46],

P.R. Pais[48], T. Pajero[28,t], A. Palano[18], M. Palutan[22], G. Panshin[78], A. Papanestis[56], M. Pappagallo[57], L.L. Pappalardo[20,g], C. Pappenheimer[64], W. Parker[65], C. Parkes[61,47], G. Passaleva[21,47], A. Pastore[18], M. Patel[60], C. Patrignani[19,e], A. Pearce[47], A. Pellegrino[31], M. Pepe Altarelli[47], S. Perazzini[19], D. Pereima[38], P. Perret[9], L. Pescatore[48], K. Petridis[53], A. Petrolini[23,h], A. Petrov[75], S. Petrucci[57], M. Petruzzo[25,q], B. Pietrzyk[8], G. Pietrzyk[48], M. Pikies[33], M. Pili[62], D. Pinci[30], J. Pinzino[47], F. Pisani[47], A. Piucci[16], V. Placinta[36], S. Playfer[57], J. Plews[52], M. Plo Casasus[45], F. Polci[12], M. Poli Lener[22], M. Poliakova[67], A. Poluektov[10], N. Polukhina[76,c], I. Polyakov[67], E. Polycarpo[2], G.J. Pomery[53], S. Ponce[47], A. Popov[43], D. Popov[52], S. Poslavskii[43], K. Prasanth[33], L. Promberger[47], C. Prouve[45], V. Pugatch[51], A. Puig Navarro[49], H. Pullen[62], G. Punzi[28,p], W. Qian[5], J. Qin[5], R. Quagliani[12], B. Quintana[9], N.V. Raab[17], R.I. Rabadan Trejo[10], B. Rachwal[34], J.H. Rademacker[53], M. Rama[28], M. Ramos Pernas[45], M.S. Rangel[2], F. Ratnikov[41,77], G. Raven[32], M. Ravonel Salzgeber[47], M. Reboud[8], F. Redi[48], S. Reichert[14], F. Reiss[12], C. Remon Alepuz[46], Z. Ren[3], V. Renaudin[62], S. Ricciardi[56], S. Richards[53], K. Rinnert[59], P. Robbe[11], A. Robert[12], A.B. Rodrigues[48], E. Rodrigues[64], J.A. Rodriguez Lopez[72], M. Roehrken[47], S. Roiser[47], A. Rollings[62], V. Romanovskiy[43], M. Romero Lamas[45], A. Romero Vidal[45], J.D. Roth[79], M. Rotondo[22], M.S. Rudolph[67], T. Ruf[47], J. Ruiz Vidal[46], J. Ryzka[34], J.J. Saborido Silva[45], N. Sagidova[37], B. Saitta[26,f], C. Sanchez Gras[31], C. Sanchez Mayordomo[46], B. Sanmartin Sedes[45], R. Santacesaria[30], C. Santamarina Rios[45], M. Santimaria[22], E. Santovetti[29,j], G. Sarpis[61], A. Sarti[30], C. Satriano[30,s], A. Satta[29], M. Saur[5], D. Savrina[38,39], L.G. Scantlebury Smead[62], S. Schael[13], M. Schellenberg[14], M. Schiller[58], H. Schindler[47], M. Schmelling[15], T. Schmelzer[14], B. Schmidt[47], O. Schneider[48], A. Schopper[47], H.F. Schreiner[64], M. Schubiger[31], S. Schulte[48], M.H. Schune[11], R. Schwemmer[47], B. Sciascia[22], A. Sciubba[30,k], S. Sellam[68], A. Semennikov[38], A. Sergi[52,47], N. Serra[49], J. Serrano[10], L. Sestini[27], A. Seuthe[14], P. Seyfert[47], D.M. Shangase[79], M. Shapkin[43], T. Shears[59], L. Shekhtman[42,x], V. Shevchenko[75,76], E. Shmanin[76], J.D. Shupperd[67], B.G. Siddi[20], R. Silva Coutinho[49], L. Silva de Oliveira[2], G. Simi[27,o], S. Simone[18,d], I. Skiba[20], N. Skidmore[16], T. Skwarnicki[67], M.W. Slater[52], J.G. Smeaton[54], A. Smetkina[38], E. Smith[13], I.T. Smith[57], M. Smith[60], A. Snoch[31], M. Soares[19], L. Soares Lavra[1], M.D. Sokoloff[64], F.J.P. Soler[58], B. Souza De Paula[2], B. Spaan[14], E. Spadaro Norella[25,q], P. Spradlin[58], F. Stagni[47], M. Stahl[64], S. Stahl[47], P. Stefko[48], S. Stefkova[60], O. Steinkamp[49], S. Stemmle[16], O. Stenyakin[43], M. Stepanova[37], H. Stevens[14], S. Stone[67], S. Stracka[28], M.E. Stramaglia[48], M. Straticiuc[36], S. Strokov[78], J. Sun[3], L. Sun[71], Y. Sun[65], P. Svihra[61], K. Swientek[34], A. Szabelski[35], T. Szumlak[34], M. Szymanski[5], S. Taneja[61], Z. Tang[3], T. Tekampe[14], G. Tellarini[20], F. Teubert[47], E. Thomas[47], K.A. Thomson[59], M.J. Tilley[60], V. Tisserand[9], S. T'Jampens[8], M. Tobin[6], S. Tolk[47], L. Tomassetti[20,g], D. Tonelli[28], D.Y. Tou[12], E. Tournefier[8], M. Traill[58], M.T. Tran[48], C. Trippl[48], A. Trisovic[54], A. Tsaregorodtsev[10], G. Tuci[28,47,p], A. Tully[48], N. Tuning[31], A. Ukleja[35], A. Usachov[11], A. Ustyuzhanin[41,77], U. Uwer[16], A. Vagner[78], V. Vagnoni[19], A. Valassi[47], G. Valenti[19], M. van Beuzekom[31], H. Van Hecke[66], E. van Herwijnen[47], C.B. Van Hulse[17], J. van Tilburg[31], M. van Veghel[74], R. Vazquez Gomez[44], P. Vazquez Regueiro[45], C. Vázquez Sierra[31], S. Vecchi[20], J.J. Velthuis[53], M. Veltri[21,r], A. Venkateswaran[67], M. Vernet[9], M. Veronesi[31], M. Vesterinen[55], J.V. Viana Barbosa[47], D. Vieira[5], M. Vieites Diaz[48], H. Viemann[73], X. Vilasis-Cardona[44,m], A. Vitkovskiy[31], V. Volkov[39], A. Vollhardt[49], D. Vom Bruch[12], A. Vorobyev[37], V. Vorobyev[42,x], N. Voropaev[37], R. Waldi[73], J. Walsh[28], J. Wang[3], J. Wang[71], J. Wang[6], M. Wang[3], Y. Wang[7], Z. Wang[49], D.R. Ward[54], H.M. Wark[59], N.K. Watson[52], D. Websdale[60], A. Weiden[49], C. Weisser[63], B.D.C. Westhenry[53], D.J. White[61], M. Whitehead[13], D. Wiedner[14], G. Wilkinson[62], M. Wilkinson[67], I. Williams[54], M. Williams[63], M.R.J. Williams[61], T. Williams[52], F.F. Wilson[56], M. Winn[11], W. Wislicki[35], M. Witek[33], G. Wormser[11], S.A. Wotton[54], H. Wu[67], K. Wyllie[47], Z. Xiang[5], D. Xiao[7], Y. Xie[7], H. Xing[70], A. Xu[3], L. Xu[3], M. Xu[7], Q. Xu[5], Z. Xu[8], Z. Xu[3], Z. Yang[3], Z. Yang[65], Y. Yao[67], L.E. Yeomans[59], H. Yin[7],

J. Yu[7,aa], X. Yuan[67], O. Yushchenko[43], K.A. Zarebski[52], M. Zavertyaev[15,c], M. Zdybal[33], M. Zeng[3], D. Zhang[7], L. Zhang[3], S. Zhang[3], W.C. Zhang[3,z], Y. Zhang[47], A. Zhelezov[16], Y. Zheng[5], X. Zhou[5], Y. Zhou[5], X. Zhu[3], V. Zhukov[13,39], J.B. Zonneveld[57], S. Zucchelli[19,e].

[1] *Centro Brasileiro de Pesquisas Físicas (CBPF), Rio de Janeiro, Brazil*
[2] *Universidade Federal do Rio de Janeiro (UFRJ), Rio de Janeiro, Brazil*
[3] *Center for High Energy Physics, Tsinghua University, Beijing, China*
[4] *School of Physics State Key Laboratory of Nuclear Physics and Technology, Peking University, Beijing, China*
[5] *University of Chinese Academy of Sciences, Beijing, China*
[6] *Institute Of High Energy Physics (IHEP), Beijing, China*
[7] *Institute of Particle Physics, Central China Normal University, Wuhan, Hubei, China*
[8] *Univ. Grenoble Alpes, Univ. Savoie Mont Blanc, CNRS, IN2P3-LAPP, Annecy, France*
[9] *Université Clermont Auvergne, CNRS/IN2P3, LPC, Clermont-Ferrand, France*
[10] *Aix Marseille Univ, CNRS/IN2P3, CPPM, Marseille, France*
[11] *LAL, Univ. Paris-Sud, CNRS/IN2P3, Université Paris-Saclay, Orsay, France*
[12] *LPNHE, Sorbonne Université, Paris Diderot Sorbonne Paris Cité, CNRS/IN2P3, Paris, France*
[13] *I. Physikalisches Institut, RWTH Aachen University, Aachen, Germany*
[14] *Fakultät Physik, Technische Universität Dortmund, Dortmund, Germany*
[15] *Max-Planck-Institut für Kernphysik (MPIK), Heidelberg, Germany*
[16] *Physikalisches Institut, Ruprecht-Karls-Universität Heidelberg, Heidelberg, Germany*
[17] *School of Physics, University College Dublin, Dublin, Ireland*
[18] *INFN Sezione di Bari, Bari, Italy*
[19] *INFN Sezione di Bologna, Bologna, Italy*
[20] *INFN Sezione di Ferrara, Ferrara, Italy*
[21] *INFN Sezione di Firenze, Firenze, Italy*
[22] *INFN Laboratori Nazionali di Frascati, Frascati, Italy*
[23] *INFN Sezione di Genova, Genova, Italy*
[24] *INFN Sezione di Milano-Bicocca, Milano, Italy*
[25] *INFN Sezione di Milano, Milano, Italy*
[26] *INFN Sezione di Cagliari, Monserrato, Italy*
[27] *INFN Sezione di Padova, Padova, Italy*
[28] *INFN Sezione di Pisa, Pisa, Italy*
[29] *INFN Sezione di Roma Tor Vergata, Roma, Italy*
[30] *INFN Sezione di Roma La Sapienza, Roma, Italy*
[31] *Nikhef National Institute for Subatomic Physics, Amsterdam, Netherlands*
[32] *Nikhef National Institute for Subatomic Physics and VU University Amsterdam, Amsterdam, Netherlands*
[33] *Henryk Niewodniczanski Institute of Nuclear Physics Polish Academy of Sciences, Kraków, Poland*
[34] *AGH - University of Science and Technology, Faculty of Physics and Applied Computer Science, Kraków, Poland*
[35] *National Center for Nuclear Research (NCBJ), Warsaw, Poland*
[36] *Horia Hulubei National Institute of Physics and Nuclear Engineering, Bucharest-Magurele, Romania*
[37] *Petersburg Nuclear Physics Institute NRC Kurchatov Institute (PNPI NRC KI), Gatchina, Russia*
[38] *Institute of Theoretical and Experimental Physics NRC Kurchatov Institute (ITEP NRC KI), Moscow, Russia, Moscow, Russia*
[39] *Institute of Nuclear Physics, Moscow State University (SINP MSU), Moscow, Russia*
[40] *Institute for Nuclear Research of the Russian Academy of Sciences (INR RAS), Moscow, Russia*
[41] *Yandex School of Data Analysis, Moscow, Russia*
[42] *Budker Institute of Nuclear Physics (SB RAS), Novosibirsk, Russia*
[43] *Institute for High Energy Physics NRC Kurchatov Institute (IHEP NRC KI), Protvino, Russia, Protvino, Russia*
[44] *ICCUB, Universitat de Barcelona, Barcelona, Spain*
[45] *Instituto Galego de Física de Altas Enerxías (IGFAE), Universidade de Santiago de Compostela, Santiago de Compostela, Spain*
[46] *Instituto de Fisica Corpuscular, Centro Mixto Universidad de Valencia - CSIC, Valencia, Spain*

[47] European Organization for Nuclear Research (CERN), Geneva, Switzerland
[48] Institute of Physics, Ecole Polytechnique Fédérale de Lausanne (EPFL), Lausanne, Switzerland
[49] Physik-Institut, Universität Zürich, Zürich, Switzerland
[50] NSC Kharkiv Institute of Physics and Technology (NSC KIPT), Kharkiv, Ukraine
[51] Institute for Nuclear Research of the National Academy of Sciences (KINR), Kyiv, Ukraine
[52] University of Birmingham, Birmingham, United Kingdom
[53] H.H. Wills Physics Laboratory, University of Bristol, Bristol, United Kingdom
[54] Cavendish Laboratory, University of Cambridge, Cambridge, United Kingdom
[55] Department of Physics, University of Warwick, Coventry, United Kingdom
[56] STFC Rutherford Appleton Laboratory, Didcot, United Kingdom
[57] School of Physics and Astronomy, University of Edinburgh, Edinburgh, United Kingdom
[58] School of Physics and Astronomy, University of Glasgow, Glasgow, United Kingdom
[59] Oliver Lodge Laboratory, University of Liverpool, Liverpool, United Kingdom
[60] Imperial College London, London, United Kingdom
[61] Department of Physics and Astronomy, University of Manchester, Manchester, United Kingdom
[62] Department of Physics, University of Oxford, Oxford, United Kingdom
[63] Massachusetts Institute of Technology, Cambridge, MA, United States
[64] University of Cincinnati, Cincinnati, OH, United States
[65] University of Maryland, College Park, MD, United States
[66] Los Alamos National Laboratory (LANL), Los Alamos, United States
[67] Syracuse University, Syracuse, NY, United States
[68] Laboratory of Mathematical and Subatomic Physics , Constantine, Algeria, associated to [2]
[69] Pontifícia Universidade Católica do Rio de Janeiro (PUC-Rio), Rio de Janeiro, Brazil, associated to [2]
[70] South China Normal University, Guangzhou, China, associated to [3]
[71] School of Physics and Technology, Wuhan University, Wuhan, China, associated to [3]
[72] Departamento de Fisica , Universidad Nacional de Colombia, Bogota, Colombia, associated to [12]
[73] Institut für Physik, Universität Rostock, Rostock, Germany, associated to [16]
[74] Van Swinderen Institute, University of Groningen, Groningen, Netherlands, associated to [31]
[75] National Research Centre Kurchatov Institute, Moscow, Russia, associated to [38]
[76] National University of Science and Technology "MISIS", Moscow, Russia, associated to [38]
[77] National Research University Higher School of Economics, Moscow, Russia, associated to [41]
[78] National Research Tomsk Polytechnic University, Tomsk, Russia, associated to [38]
[79] University of Michigan, Ann Arbor, United States, associated to [67]

[a] Universidade Federal do Triângulo Mineiro (UFTM), Uberaba-MG, Brazil
[b] Laboratoire Leprince-Ringuet, Palaiseau, France
[c] P.N. Lebedev Physical Institute, Russian Academy of Science (LPI RAS), Moscow, Russia
[d] Università di Bari, Bari, Italy
[e] Università di Bologna, Bologna, Italy
[f] Università di Cagliari, Cagliari, Italy
[g] Università di Ferrara, Ferrara, Italy
[h] Università di Genova, Genova, Italy
[i] Università di Milano Bicocca, Milano, Italy
[j] Università di Roma Tor Vergata, Roma, Italy
[k] Università di Roma La Sapienza, Roma, Italy
[l] AGH - University of Science and Technology, Faculty of Computer Science, Electronics and Telecommunications, Kraków, Poland
[m] LIFAELS, La Salle, Universitat Ramon Llull, Barcelona, Spain
[n] Hanoi University of Science, Hanoi, Vietnam
[o] Università di Padova, Padova, Italy
[p] Università di Pisa, Pisa, Italy
[q] Università degli Studi di Milano, Milano, Italy
[r] Università di Urbino, Urbino, Italy
[s] Università della Basilicata, Potenza, Italy
[t] Scuola Normale Superiore, Pisa, Italy
[u] Università di Modena e Reggio Emilia, Modena, Italy
[v] Università di Siena, Siena, Italy

[w] *MSU - Iligan Institute of Technology (MSU-IIT), Iligan, Philippines*
[x] *Novosibirsk State University, Novosibirsk, Russia*
[y] *Sezione INFN di Trieste, Trieste, Italy*
[z] *School of Physics and Information Technology, Shaanxi Normal University (SNNU), Xi'an, China*
[aa] *Physics and Micro Electronic College, Hunan University, Changsha City, China*

[†] *Deceased*

,